國立臺灣大學醫學院暨工學院醫學工程學研究所

碩士論文

Graduate Department of Biomedical Engineering

College of Medicine and College of Engineering

National Taiwan University

Master Thesis

藉由輻射刺激探討真皮層中的巨環境影響毛囊再生

Dermal macroenvironment promote hair regeneration in adaptation to irradiation dystrophy

鄭學瀛

Suet Yee Tee

指導教授：林頌然 博士

Advisor: Sung-Jan Lin, M.D. & Ph.D

中華民國 108 年 6 月

June, 2019

doi:10.6342/NTU201901903

口試委員審定書

國立臺灣大學碩士學位論文
口試委員會審定書

藉由輻射刺激探討真皮層中巨環境與毛囊再生關係
Dermal macroenvironment promote hair regeneration in adaptation to irradiation dsytrophy

本論文係鄭學瀛（學號 R06548060）在國立臺灣大學醫學工程學系完成之碩士學位論文，於民國 2019 年 6 月 26 日承下列考試委員審查通過及口試及格，特此證明

口試委員：林俊宏

（指導教授）

_____ _____

_____ _____

_____ _____

_____ _____

系主任：黃義侑

1

doi:10.6342/NTU201901903

Acknowledgement

在醫工所的這兩年碩士生涯，可以說長不長，短也不短。在這段時間裡，時間過得很充實，讓我在研究路上獲益匪淺，也讓我留下許多深刻回憶。在研究旅程上，實驗並非能一直如願般的一帆風順，事實上容易遇到許多瓶頸期。感謝實驗室的大家，在我遇到瓶頸期的同時，給予我許多建議與幫助，讓我順利度過關卡。在此由衷感謝大家的幫忙與指教！

在此誠摯感謝指導教授林頌然老師指導與提供自由度，讓我在研究過程中能繼續保持追求新知的熱忱。希望在未來的旅程中，能繼續保持求知若渴的精神，接受面對未來的挑戰。

鄭學瀛 謹誌於

台灣大學醫學工程所

中華民國 108 年 8 月 6 日

doi:10.6342/NTU201901903

中文摘要

根據 WHO 在 2018 年統計指出，癌症是全球第二大死因，約占整體死因的六分之一。每種類型的癌症有不同的治療方式，包括：外科手術、化學治療、放射治療。然而，藉由放射治療對於局部的癌細胞進行毒殺，其所造成的副作用較嚴重，例如：皮膚會出現潮紅、乾燥、發癢，或是疲倦、食慾減低，甚至是局部照射範圍有掉髮的現象。

皮膚是哺乳動物最大的器官系統，而毛囊是動態微小器官並且深入生長於皮膚真皮層中，作為微小器官的毛囊，有著規律的生長週期，包含：生長期、凋亡期、休止期。各時期的毛囊均會有不同的結構或是細胞組成；而圍繞著毛囊的巨環境，例如有：神經、血管、脂肪組織等。除此之外，在毛囊內亦有幹細胞的分佈以維持毛髮週期不斷的循環再生。然而，生長期的毛囊若接受放射治療、輻射傷害後，會使毛囊進入萎縮性生長期或是萎縮性衰退期。

本實驗室先前的研究已發現毛囊在不同輻射劑量刺激下，會促使毛囊進入不同程度的衰退期。本研究的目的為探討輻射刺激後真皮層的巨環境與毛囊再生的關係，以期能瞭解輻射刺激後之毛囊再生機轉。實驗以輻射劑量 2 Gy 與 5.5 Gy 誘導毛囊進入適應性衰退期。毛囊在 5.5 Gy 輻射刺激後會有萎縮的現象，而在稍後恢復形態；而肌肉纖維與膠原纖維也因 5.5 Gy 輻射刺激後發生皺縮的現象，且此現象的改變與毛囊衰退期時間相吻合。我們以質譜定序且定量輻射後真皮層細胞的蛋白質，以期能從中獲得毛囊再生的相關資訊。從定序結果中發現，脂肪代謝相關蛋白在總蛋白質中有顯著的差異。最後，我們以 5.5 Gy 輻射處理小鼠後，餵食脂肪溶解抑制劑，以驗證脂肪溶解在毛囊再生中扮演的角色。實驗結果顯示，餵食脂肪溶解抑制劑的小鼠，其毛囊會延遲再次進入生長期約 10 天。

doi:10.6342/NTU201901903

總結以上的實驗結果，本研究驗證了真皮層巨環境中之脂肪代謝在輻射刺激後之毛囊再生扮演重要的角色，脂肪代謝對於輻射刺激後之毛囊再生不可或缺。

關鍵字：放射治療、掉髮、毛囊再生、脂肪代謝

doi:10.6342/NTU201901903

Abstract

According to WHO organization report, cancer is the second highest cause of death, accounting for approximately one sixth of death incidence in the world. There are several types of cancer treatments depending on the type of cancer and how advanced it is. Examples of current methods include chemotherapy, radiotherapy and surgery. A localized radiotherapy treatment, utilizing low doses or high doses of radiation to kill cancer cells, often causes a variety of side effects such as itchy skin, tiredness and temporary localized hair loss.

Skin is the largest organ in mammals. The hair follicle(HF) is one of the characteristic features of mammals serves as a unique mini-organ, anchoring into the skin. The hair follicle keeps regular hair growth cycle in three different stages: anagen, catagen and telogen stages. Each stage has different hair structures,cell populations, and macroenvironment in dermis. In addition, there are stem cells distributed in hair follicle in order to sustain hair cycle regeneration. Hair follicles would enter either dystrophy anagen or dystrophy catagen if the hair follicles are exposed to long term radiation during a radiotherapy.

Our lab's previous studies indicated 2 Gray (Gy) and 5.5 Gy ionizing radiation may induce hair dystrophy in different manners. The aim of this study is to figure out the relationship between dermal macroenvironment and hair regeneration in adaptation

doi:10.6342/NTU201901903

to irradiation dystrophy, and to understand the mechanism of hair follicle regeneration upon radiation damage. In this study, HFs in 5.5Gy ionizing radiation will degenerate and recover afterwards. Afterwards, dermal macro-environment will be dramatically changed as seen in immunostaining of oil red O(ORO) and Masson trichome staining after radiation treatment. Thus, we utilized mass spectrometry to identify and quantify protein expression in dermal macroenvironment after ionizing radiation. Based on protein sequencing data, it indicates that proteins associated with fatty acid metabolism would be changed significantly after radiation. Finally, we used Acipimox (lipolysis inhibitor) as our functional assay for animal model to confirm that lipolysis plays the important role in hair regeneration after ionizing radiation. The results indicated that HFs would delay re-entering of anagen stage almost 10 days, comparing with no-drug intake control group. In summary, our findings revealed that fatty acid metabolism of dermal macroenvironment would be a vital factor of hair regeneration after ionizing radiation. Thus, we believe that fatty acid is essential for hair follicle regeneration stimulated by ionizing radiation.

Keywords：radiotherapy, hair loss, hair follicle regeneration

doi:10.6342/NTU201901903

List of abbreviations

1.	RT	Radiation treatment
2.	HFs	Hair follicles
3.	HS	Hair shaft
4.	IR	Ionizing radiation
5.	DWAT	Dermal white adipose tissue
6.	ORO	Oil red O

doi:10.6342/NTU201901903

Contents

doi:10.6342/NTU201901903

doi:10.6342/NTU201901903

LIST OF FIGURES

doi:10.6342/NTU201901903

Chapter1 Introduction

1.1Introduction to radiation

Radiation known as the energy emanated by waves or energized particles and its propagation of energy transmitted through space or matter. (Mehta, Suhag et al. 2010) Radiation can destroy living cell's DNA by breaking down chemical bonds of between molecules and modify cellular structure of organism. These damages are at the cellular level and hence effect of exposure to radiation is difficult to detect. (Donya, Radford et al. 2014) Radiation has various basic physical forms such as electromagnetic waves, energetic particles or both. Electromagnetic radiation includes of waves of oscillating electrical and magnetic fields, which is pure energy with no weight like radio waves. electromagnetic radiation spectrum includes x-rays, visible light, infrared light, and radio waves. (Balagamwala, Stockham et al. 2013) Particle radiation used in therapy can be divided into 2 categories: "proton-therapy" characterized by low linear energy transfer (LET) and "heavy-ion therapy" with high LET properties. (Schulz-Ertner, Jakel et al. 2006) Usage of radiation in therapy is due to the biophysical and biological superiority of particle beam. Proton and heavier ion beams are included in the particle beams. It's energy given off during penetration depth of matter called *bragg peak*.(Brown and Suit 2004) Its has better treatment localization compared to photon beams. Thus treatment can be perform without

doi:10.6342/NTU201901903

inducing toxicity in normal tissues in close proximity.

doi:10.6342/NTU201901903

1.2 Clinical applications of radiation and its biological effect on mammal

Cancer become a leading cause of death in developed countries. Surgery has been the most effective treatment for cancer therapy until the advent of radiotherapy in the 1920s and chemotherapy after 1940s. (A. Urruticoechea 2010) In contrast to surgery, chemotherapy has systemic side effects for treatment and radiotherapy locally affects normal tissues in proximity to the targeted tissue.(Bentzen, Dorr et al. 2003)) There are several types of ionizing radiation therapy against cancer, including x-rays, gamma rays, electron beams.(Teruhiko Terasawa 2009) Radiation has since been widely used to treat certain types of cancers in the late 19th century. Cancer cell exposed to I.R. will undergo various types of cell death through cytotoxic lesions. The types of cell death include apoptosis, mitotic catastrophe, necrosis, senescence, autophagy.(Baskar, Lee et al. 2012) Although the advantage of radiation therapy is a localized treatment for targeted cell, I.R. also induces systemic effects as side effect.(Formenti and Demaria 2009)

doi:10.6342/NTU201901903

1.3 Hair follicle and dermal macroenvironment

HFs can continuously go through cyclic growth life and apoptosis, including active phase(anagen), dystrophic phase(catagen), rest phase(telogen).(Alonso and Fuchs 2006) In murine model, hair cycle will synchronized with dermal white adipose tissue. Increasing size of dermal white adipose tissue (DWAT) in dermis will always coincide with growth life of hair follicle.(Foster, Nicu et al. 2018) Structure of HFs in each hair cycle stage is diverse. (Paus 2001) However, DWAT changes alongside of Hfs in dermis. (Arnold Biological Luboratory 1953)

1.3.1 Structure of hair follicles

HFs grow beneath the skin surface and has differentiated organelles with cylindrical structure, including sebaceous gland, bulge, outer root sheath(ORS), inner root sheath(IRS), medulla, hair bulb and dermal papilla cells(DPCs).(Schneider, Schmidt-Ullrich et al. 2009) HFs have concentric layers ofcells surrounding central of hair shaft.Outer root sheath(ORS) is localized at the outer most layer. There are several types of keratins, adhesion molecules, cytokines, and growth factors receptors present as well. ORS can regenerate after receiving injury or stimulation.(Franklin H. Epstein 1999) Adjacent to hair shaft is the inner root sheath(IRS). IRS contains different fibrillar proteins and represents a rigid cylinder at the lower part of HFs.(Hardy 1992) At the base of HFs is hair bulb that containing adult tissue stem

doi:10.6342/NTU201901903

cells residing in niches known as hair matrix. These cells have short lifespan and then differentiate into other lineages. (Yang, Adam et al. 2017) The Hair matrix embraces a pocket of mesenchymal cells called dermal papilla(DP) that thought to be a reservoir of multi-potent stem cells. (Driskell, Clavel et al. 2011)

1.3.2 Hair cycling

During cyclic life of degeneration and regeneration known as hair cycle, HFs consist of three periodic stages, which are growth phase(anagen), dystrophic phase(catagen), resting phase(telogen).(Alonso and Fuchs 2006) Inhibitor or stimulator will affect HFs cyclical change activity such as flux from cycle to cycle.(Davis 1962) **Anagen** is a growth phase that can be divided into six substages.(Herman B. Chase 1951) Anagen VI stage is distinct from other stages in that it has the maximum rate of hair growth.(Chase 1954) In this stage, bulge stem cell and 2nd hair germ will differentiate into other concentric layer cell types.(Greco, Chen et al. 2009) **Catagen** is regarded as a transitional stage where HFs is converted from an active phase to a resting phase.(Chase 1954) There is a massive keratinocyte apoptosis occurring in the hair bulb but dermal papilla is unaffected.(GerdLindner 1997) **Telogen** is the quiescence stage. HFSCs in this stage enter resting phase and wait for the next anagen stage.(Stenn KS 1999) Telogen HFs is surrounded by

doi:10.6342/NTU201901903

interfollicular dermal fibroblasts and reach its minimum length relative in the hair cycle.(Muller-Rover, Handjiski et al. 2001)

1.3.3 Structure of dermal macroenvironment

When the skin organ is fully grown it will integrate with white adipose tissue that comprises unilocular adipocytes to store fatty acids for energy.(Driskell, Jahoda et al. 2014) Much research in recent years has focused on the relationship between adipocyte lineage cells and the hair cycle. For example, Horsley *et al.* showed that dynamic regeneration of adipocyte precursor cells could be parallel to the activation of skin stem cells. However, adipogenesis defection would affected follicular stem activation.(Festa, Fretz et al. 2011) Another study showed that dermal adipose tissue will undergoe morphology changed and induce HFs cycle.(Foster, Nicu et al. 2018) (Fig.1)

1.3.4 Adipose tissue

Adipose tissue have always had the biological role of immunity and inflammation in animal. The major white adipose tissue depot is found at the subcutaneous region of abdominal or gluteal-femoral.(Kwok, Lam et al. 2016) In mice skin, dermal white adipose tissue is a continuous layer. It can be separated into

doi:10.6342/NTU201901903

DWAT and subcutaneous dermal white adipose tissue. which are divided by the panniculus carnosus.(Zwick, Guerrero-Juarez et al. 2018) There are various cell types in adipose tissue, including adipocytes, vascular cells, neuronal cells, immune cells, extracellular matrix and stromal cells. But, the main component in adipose tissue is mature adipocytes.(Lago, Cerqueira et al. 2018) (Fig.2)

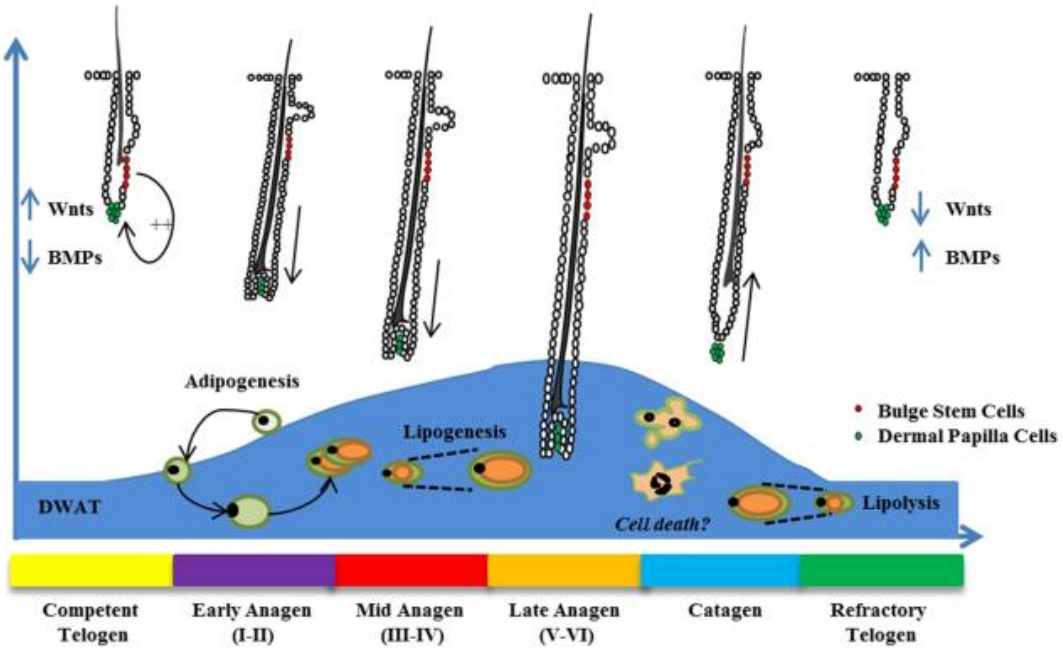

Fig.1 Murine HC-dependent DWAT fluctuations(April R. Foster et al. 2018) This illustration reveal that hair cycling may parallel with DWAT fluctuations.

doi:10.6342/NTU201901903

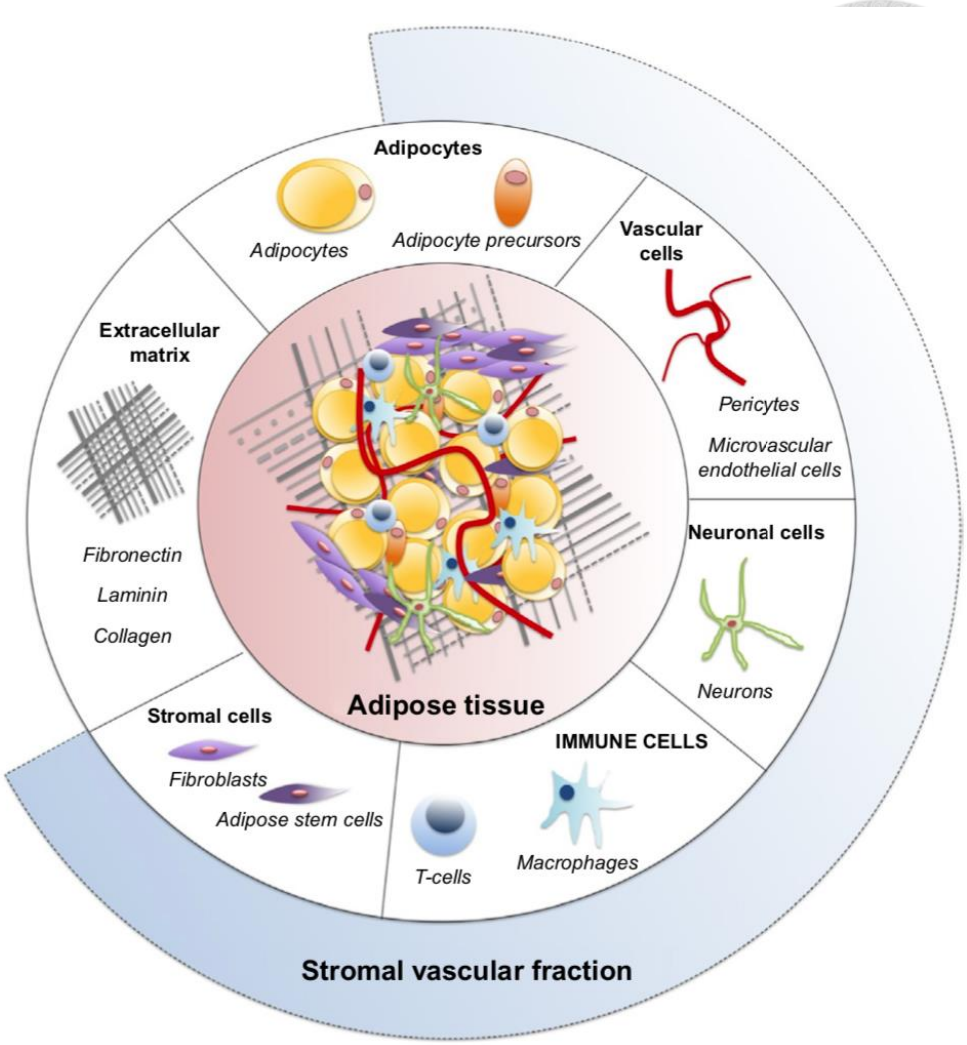

Fig.2 Adipose tissue components. (Lago, Cerqueira et al. 2018) Adipose tissue is a complex endocrine organ. Adipose tissue include adipocytes, extracellular matrix, stromal cells, immune cells, neuronal cells, and vascular cells.

doi:10.6342/NTU201901903

1.4 Response of hair follicle to ionizing radiation

In previous study, chemotherapy and radiotherapy are widely used in cancer treatment.(Delaney, Jacob et al. 2005) Although radiotherapy is a non-invasive therapy but is associated with various side effects depending on radiation dosage and particle beam types.(Bentzen 2006) HFs are highly proliferative and sensitive organs that can easily acquire genotoxic injuries via ionizing radiation.(F.D. Malkinsonm 1972) The common clinical side effects of radiotherapy toxicity are acute gastrointestinal(GI) damage, cardiac toxicity, cognitive impairment, reproductive disorders and hair loss.(De Ruysscher, Niedermann et al. 2019) Numerous researchers are attempting to find out strategies to prevent hair loss by radiotherapy. Until now, there is no effective strategy to cure hair loss induced by ionizing radiation. It is more important to figure out how HFs regeneration is induced by ionizing radiation. Normally, the human HFs are in the anagen stage 90% of the time. Human may suffer hair loss after receiving radiation therapy due to hair matrix cells' highly proliferative and sensitive nature during anagen stage.(Foitzik, Krause et al. 2006) In the previous study, it is shown that HFs might have different hair repair responses to chemical drug.(Fig.3) Hence, understanding the response of HFs toward radiation is extremely important in Pathobiology (Paus, Haslam et al. 2013)

doi:10.6342/NTU201901903

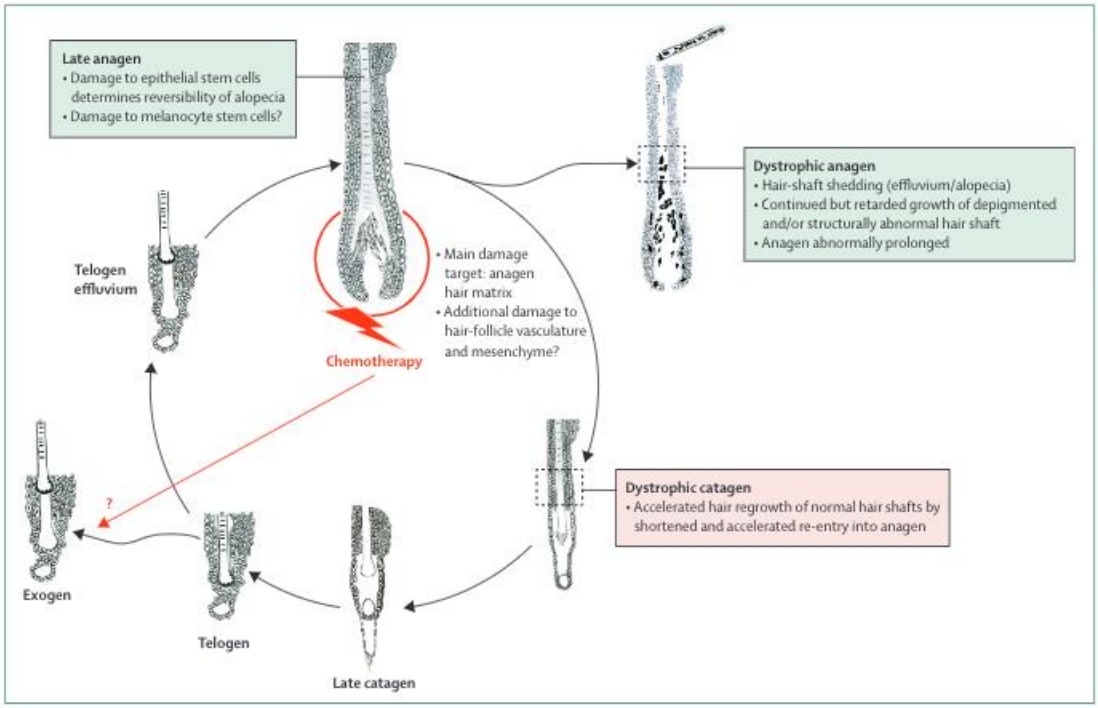

Fig.3 Two repaired pathways of HFs induced by chemotherapy. (Paus, Haslam et al. 2013) Two approaches to repair HFs induced by chemotherapy.

doi:10.6342/NTU201901903

1.5 Motivation and purpose

For cancer patients, hair loss may be a side effect of chemotherapy or radiotherapy. Managing hair loss is an important part of cancer care and treatment. In this study, we try to figure out the relationship between dermal macro-environment and hair regeneration in adaptation to irradiation dystrophy.

doi:10.6342/NTU201901903

Chapter 2 Materials and methods

2.1 Animals

Mice

C57BL/6 female mice of 4 weeks old age were purchased from Taiwan National Laboratory Animal Center(Tainan, Taiwan). All animals were prepared in accordance with Institutional Animal Care and Use Committee of National Taiwan University.

Laboratory animal anesthesia

In animal studies, anesthetic agents is prepared with a mixture of 5ml zolazepam (Zoletil vet, Virbac Laboratories) , 3.75ml saline and 1.25ml Rompun (Bayer, Germany) for intramuscular injection.

BrdU labeling

For proliferating cell observation, we performed intraperitoneal injection of 1mg of 5-bromo-20-deoxyuridine (BrdU) 1 hour before skin samples were collected.

doi:10.6342/NTU201901903

2.2 Mass Spectrometry work flow

2.2.1 Tissue lysis

After receiving radiation treatments, mice dermal tissues were scraped off by scalpel. Promptly, these tissues were collected into Eppendorf and stored in liquid nitrogen for further processing. After measurement of dry weight, PTS-lysis buffer (12nM SDC, 12mM SLS in 100mM Tris-HCL, pH9.0 with protease inhibitor cocktail and phosphatase inhibitors) was added to sample. Then, the homogenization was performed with pestle tube homogenizers under 4℃ before the centrifugation under 16000 r.c.f., 30 minutes, 4℃. Later, samples in extracted supernatant were measured for protein concentration and quantification with bicinchoninic assay(BCA). Proteins was purified by chloroform-methanol precipitation and dissolved in 8M urea for denaturing.

2.2.2 BCA assay

Pierce^{TM} BCA protein kit composed of reagent A and reagent B were used to examine the quantification of protein. Reagent A consists of sodium carbonate, sodium bicarbonate and sodium tartrate in 0.1N sodium hydroxide. Reagent B consists of copper(II) sulfate solution. Combination of buffer A and buffer B with ratio 50:1(vol/vol) is used to prepared BCA solution. Standard calibration curve was

doi:10.6342/NTU201901903

prepared from BSA dissolving in BCA solution to form concentration of 0μg/mL, 2 μg/mL, 4 μg/mL, 6 μg/mL, 8 μg/mL, 10 μg/mL.

2.2.3 Protein digestion

For reduction, DTT at 10mM final concentration was added in the sample and placed on shaker for 29℃, 30mins for sufficient amalgamation. For alkylation, IAM at 50mM IAM for final concentration were infused into the sample for 29℃, 30mins. After dilution by urea 1M, denatured proteins were digested with LysC in protein-enzyme ratio 100:1 for 4 hours, 29℃, then with trypsin in protein-enzyme ratio 50:1 overnight at 29℃.

2.2.4 SDB-XC-stage tip desalting

SDB-XC is a sample preparation tip column that used to desalt and enrich peptides. To accomplish salting, we first had to complete protein digestion, kinase reaction and IMAC enrichment. SDB-XC (Styrene Divinylbenzene) bead is packed into stage-tip, thenwashed using 80%ACN as an ctivation agent based on condition with 0.5%ACN. At the end, used 80%ACN to elute and transfer the peptides into a new tube.

doi:10.6342/NTU201901903

2.2.4 LC-MS/MS analysis

Suspension of sample are done using 0.1% FA (formic acid) for analysis. Thermo LTQ-Orbitrap Fusion Lumos Tribrid mass spectrometer system (Thermo Fisher Scientific, San Jose, SA) with an Ultimate 3000 RSLCnano system (Thermo Fisher Scientific, San Jose, SA) is used for mass spectrometry analysis. The 75μmx50cm analytical column of RSLCnano system is collected with 3μm C_{18} particles. The buffer system is combined with 0.1%FA (buffer A) and CAN with 0.1% FA(buffer B). The LC gradient is 150mins gradient at 0.5 nL/min flow speed. The range of each full MS scan is around 400m/z to 1650m/z and is accompanied with 15 data dependent acquisition (DDA). Later, dynamic exclusion setting accorded to charge states positive2-5, exclusion duration 20s, injection time 50ms. At the end, HCD is allowed for collision scanning: isolation window 1.6m/z, AGC target 1.0x 10^5, HCD collision energy 27%, orbitrap resolution 15000.

2.2.5 Database search and quantitation

We use MaxQuant software to handle LC-MS/MS data.(Cox and Mann 2008) Label-free quantification (LFQ) algorism is utilized for quantification. The standard parameters of peptide modification are $^{13}C_6$-L-Lysine, $^{13}C_6{}^{15}N_4$-L-Arginine in

doi:10.6342/NTU201901903

SILAC, carbamidomethyl(C), ^{16}O-phospho(STY), ^{18}O-phospho(STY), acetyl(N-term), deamidation(NQ) are oxidation(M) are set in Maxquant.

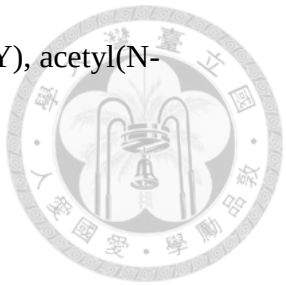

doi:10.6342/NTU201901903

2.2.6 Chemical material for protein quantification

Chemical and materials	Sources
Acetonenitrile	Merck
Acetonitrile-0.1% Formic acid	J.T.Baker
Acetic Acid	Merck
Acrylamide solution (40%,37.5:1)	Bio-Rad
Ammonium Hydroxide	Sigma
Ammonium persulfate(APS)	Amersham Pharmacia
BCA^{TM} Protein Assay Kit	Thermofisher
BSA	Sigma
$^{13}C_6{}^{15}N_4$ L-Arginine-HCl	Thermofisher
$^{13}C_6{}^{15}N_2$ L-Lysine-2HCl	Thermofisher
CK2 recombinant kinase	NEB
Dithiothreitol	Sigma
EDTA	Merck
Ethanol	Merck
Formic acid	Riedel
Glycine	J.T.Baker
Iodoacetamide	Sigma
Lys-C	Sigma
Methanol	Merck
Milli-Q Ultrapure Water Purification System	Millipore
N,N,N', N'-Tetramethylenediamine(TEMED)	Amersham Pharmacia
Ni-NTA silica resin	Qiagen
Protease inhibitor cocktail	Roche
SDB-XC Empore disk	3M
Stage-Tip	Gilson
Tris-HCl	Sigma
Triethylammonium bicarbonate	Sigma
Trifluoroacetetic acid	Sigma
Trypsin	Promega
Tween 20	Sigma
Urea	USB Corporation
Water	Milli-Q system
Water-0.1% Formic acid	J.T.Baker

doi:10.6342/NTU201901903

2.3 Irradiation treatment

Female mice at postnatal day21 was shaved carefully with electric shaver. Around 7 to 10days later, we checked that dorsal skin was color in black and dorsal HFs entered early full anagen stage. Each mice were then anesthetized, and the mouse received single doses(2 or 5.5Gy) of γ irradiator by ^{137}Cs source on the dorsal side.(dosage: 3.37Gy/minute, γ irradiator IBL 637 from CIS Bio international). Mice were all irradiated in the morning.

2.4 Histology examination

Mouse skin samples were collected and fixed with 4% paraformaldehyde at 4℃ overnight. Subsequently, these tissues were embedded in paraffin wax and $5\mu m$ sections were used for hematoxylin and eosin staining.

2.5 Pharmaceutical lipolysis inhibition

Lipolysis inhibitor, Acipimox, was purchased department of pharmacy of National Taiwan University Hospital. Acipimox (75mg/Kg) oral intake was administrated before 3days IR treatment. In the 25 following days, mice received Acipimox daily. Phenomenon of hair loss were observed within 60 days post

doi:10.6342/NTU201901903

exposure to IR treatment. (LD50 values in mice and rats range from 2000 to 5000mg/Kg)

2.6 Immunofluorescence staining and microscopy

The mouse skin samples were fixed with 4% paraformaldehyde(PFA) at 4℃ overnight. Then they are dehydrated and embedded by OCT or paraffin wax. Paraffin sections were dewaxed using xylene and rehydrated for antigen retrieval process. We use citrate buffer(**10mM Citric acid, 0.05% Tween20, pH6.0)** as the antigen retrieval buffer and heat up to 95℃. Then, we put in our sections with citrate buffer at 95℃ for 20 minutes. Afterwards, 5% BSA is used as the blocking buffer, the primary antibodies used were rat anti-BrdU (abcam, 1:100), rabbit anti-cleaved caspase3(cell signaling, 1:100), rat F4/80 (abcam6640, 1:100), CD31 (abcam56299, 1:100). The following secondary antibodies were Alexa Fluor Cy3-conjucated donkey anti-rabbit IgG (H+L) (Jackson Immuno Research, 712-165-153, 1:300) and Alexa Fluor 488-conjucated donkey anti-rat IgG (H+L) (Jackson Immuno Research, 711-165-152, 1:300)

doi:10.6342/NTU201901903

2.7 Oil red O staining

The frozen section of mouse skin specimen were fixed with 4% paraformaldehyde(PFA) at 4℃ overnight and soon and embedded in OCT. Afterwards, we used PBS to dissolve OCT agent and then dipped samples in 60% isopropanol for 15 minutes. Next, samples were stained in working Oil red O solution for 15 minutes. Subsequently, the sections were dipped into 60% isopropanol again and for 15 minutes. Lastly, used 50% glycerol as mounting medium and covered the sample for microscope observation.

2.8 Statistical analysis

To reduce within-group variance, two radiation dosage proteomic group by group comparison were done with one way-ANOVA analysis. The difference between group was considered statistically significant when $p<0.05$. All statistical comparison group of staining were performed by software Prism (GraphPad).

doi:10.6342/NTU201901903

Chapter 3 Results

3.1 Hair follicle respond to ionizing radiation

In this experiment, we sought to clarify effect of ionizing radiation to dermal macroenvironment and hair follicle. Prior to ionizing radiation treatment, an animal model needed to be established. At the beginning, C57BL/6 female mice dorsal skin were irradiated at 32 days of age with gamma radiation from Cs-137 irradiator. Before getting 2Gy and 5.5Gy ionizing radiation exposure, mouse were shaved at the dorsal region to make sure hair cycle in full anagen stage. If dorsal skin of mice is color in black, mice are in anagen VI stage. As can be seen, there was no significant changes in the following day after 2Gy radiation. But, there was significant hair loss at post-5.5Gy irradiation day5 when compared with the non-irradiated control mice as indicated in Fig.4a. It may be reasonable to rationalize that hair loss is caused by higher dose of ionizing radiation. There was a notable difference between post-5.5gy I.R. day4 and non-I.R. day4 mice as shown in Fig.4b.

doi:10.6342/NTU201901903

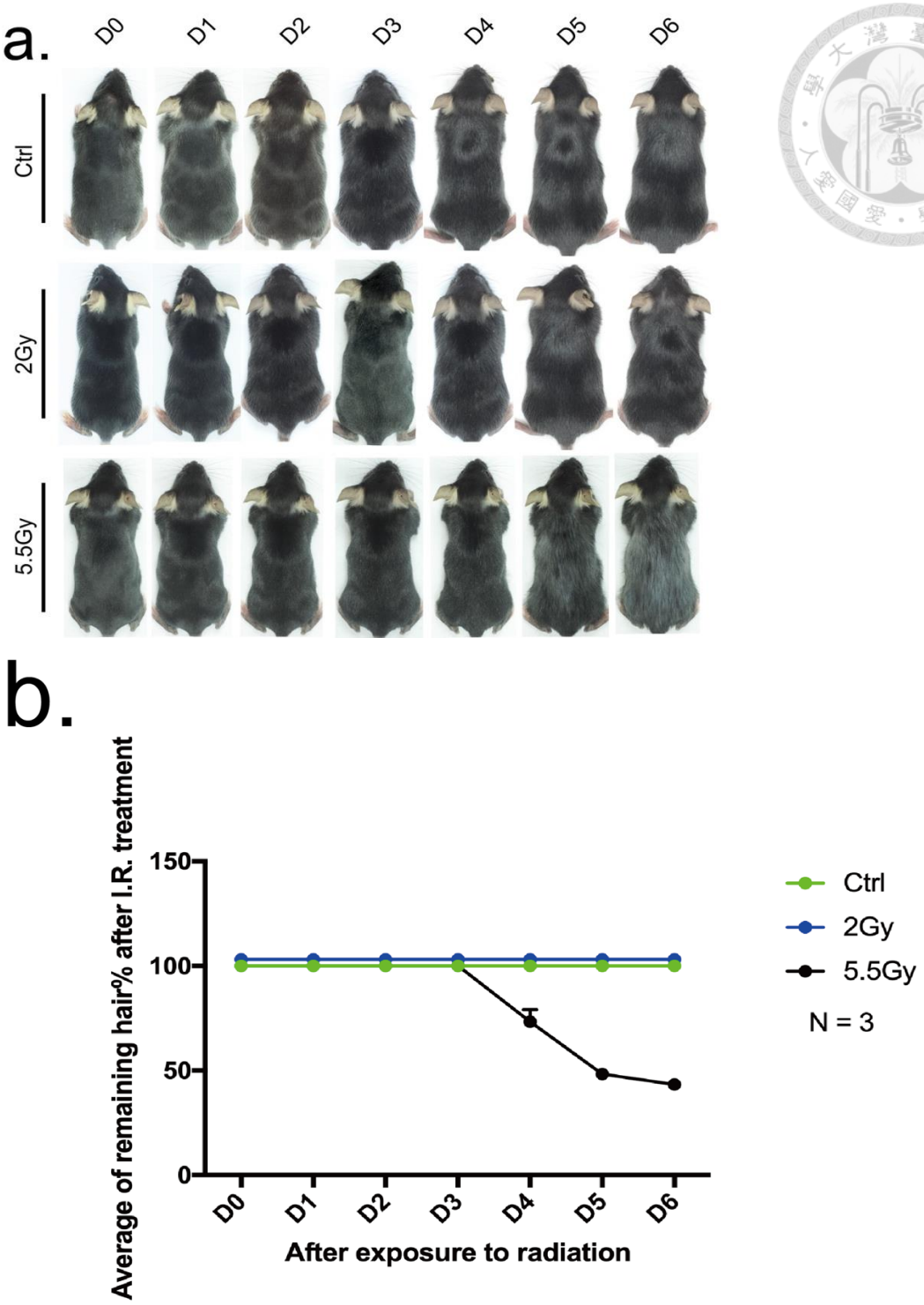

Fig. 4 Ionizing radiation induce hair loss.

(a) Gross phenomenon of hair growth was performed in non-radiation(control), 2Gy radiation, 5.5Gy radiation. Mice receiving 5.5Gy radiation were more significant and would get hair loss than 2Gy radiation.

(b) Hair growth score after exposure to ionizing radiation

doi:10.6342/NTU201901903

3.2 Irradiation trigger dermal macroenvironment change

From the phenomenon described above, we obtained reliable evidence showing dose-dependent HF loss. The evidence points to the likelihood that hair follicle dystrophy caused hair loss. Hence, we examined hair follicle dystrophy in H&E staining. It displayed that dermal macroenvironment and hair follicle had no any significant diversity in non-irradiation group. The structure of hair follicle and dermal macroenvironment remains intact. It was also evident that non-irradiation group and exposure to 2Gy group are alike. Dermal macroenvironment and hair follicle exposed to 2Gy irradiation would not change its morphology. However, there were significant decrease in the thickness ratio of skin and hair follicle dystrophy at post-5.5Gy I.R. day3. (see Fig.5b) In the meantime, it can be seen that melanin migrated from medulla to outer root sheath. There also a tendency for dermal white adipose tissue to decrease in size congruently with 5.5Gy I.R. induced hair dystrophy. Shortly after the hair dystrophy, injured hair bulb began to restore its structure at post-I.R. day5. It can be observed that dermal macroenvironment highly correlated with hair regeneration. Nevertheless, there is considerable disparity in the behavior of hair follicle after exposure to 2Gy and 5.5Gy irradiation. Based on this information, we speculated 2Gy irradiation caused lower damage compared to 5.5Gy irradiation. We therefore

doi:10.6342/NTU201901903

speculate that injury caused by 2Gy irradiation recovered within 24 hours post irradiation.

doi:10.6342/NTU201901903

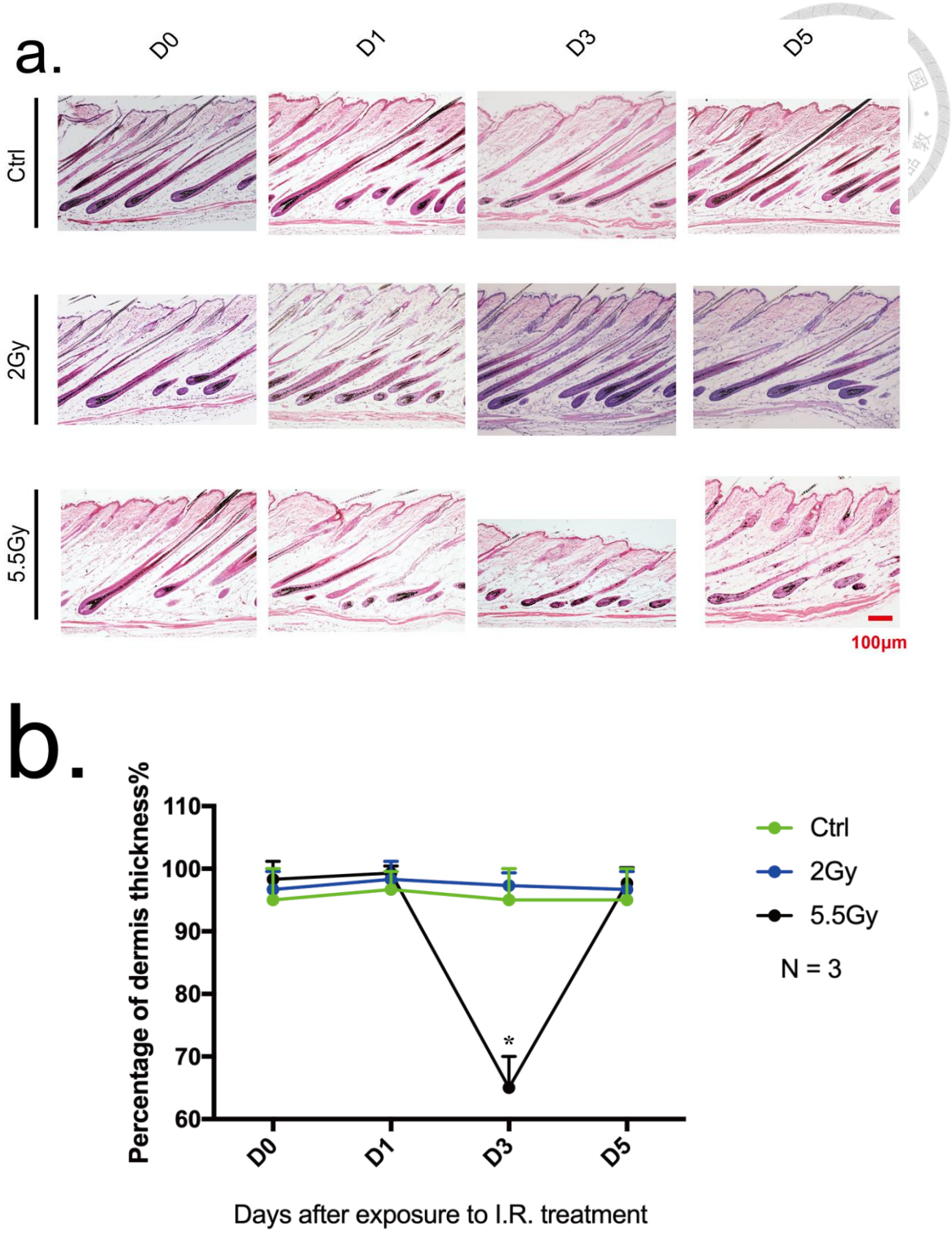

Fig.5 Histology examination of dorsal skin exposure to 2Gy and 5.5Gy I.R. treatment. (a) Histology of dermal macroenvironment after exposure to radiation. This results indicated that thickness of skin would get thinner compared to other conditions. (b) Thickness of dermal macroenvironment after exposure to radiation.

doi:10.6342/NTU201901903

3.3 Irradiation induce hair injury in dermal macroenvironment

In biology, most organisms response to stress or stimulation which led to injuries always resulted in cell apoptosis. The purpose of these natural phenomenon are to maintain homeostasis between cell death and cell renewal.(Porter AG1 1999) In the previous study, Ralf Paus etc. defined that phenotypes of hair follicle from anagen to catagen were natural cell apoptosis.(Muller-Rover, Handjiski et al. 2001, Pawlik and Keyomarsi 2004). As mentioned previously, the aim of this study was to determine how irradiation would induce hair follicle injury.. It isn't likely any difference by the distribution of cell proliferation at day0 to day5 in non irradiation group. Furthermore, we studied that there is no cleaved-caspase3 positive staining cell in the result. In the previous study, if HFs are exposured to 2Gy radiation, cell death progress will happen in 24hrs. However, HFs cell death induced by 5.5Gy radiation also appeared at 24hrs.(Huang, Lai et al. 2017) Thus, two dosage radiation induced HFs cell death mainly display before 24hrs. As can be seen in Fig.6a&6c, cleaved caspase3 positive cells only expressed at post-5.5Gy I.R. day1. Afterward, there wasn't any cell proliferation at post-5.5Gy I.R. day3. As evident in Fig.6b, if hair follicle is exposed to 5.5Gy I.R., cell proliferation will significantly decreased and the lowest appeared at day3. In addition, cell proliferation activity would increase at day5 after exposure to

doi:10.6342/NTU201901903

2Gy and 5.5Gy I.R. This result implied that hair follicle were highly sensitive to both 2Gy and 5.5Gy I.R. and recovered later in both cases.

doi:10.6342/NTU201901903

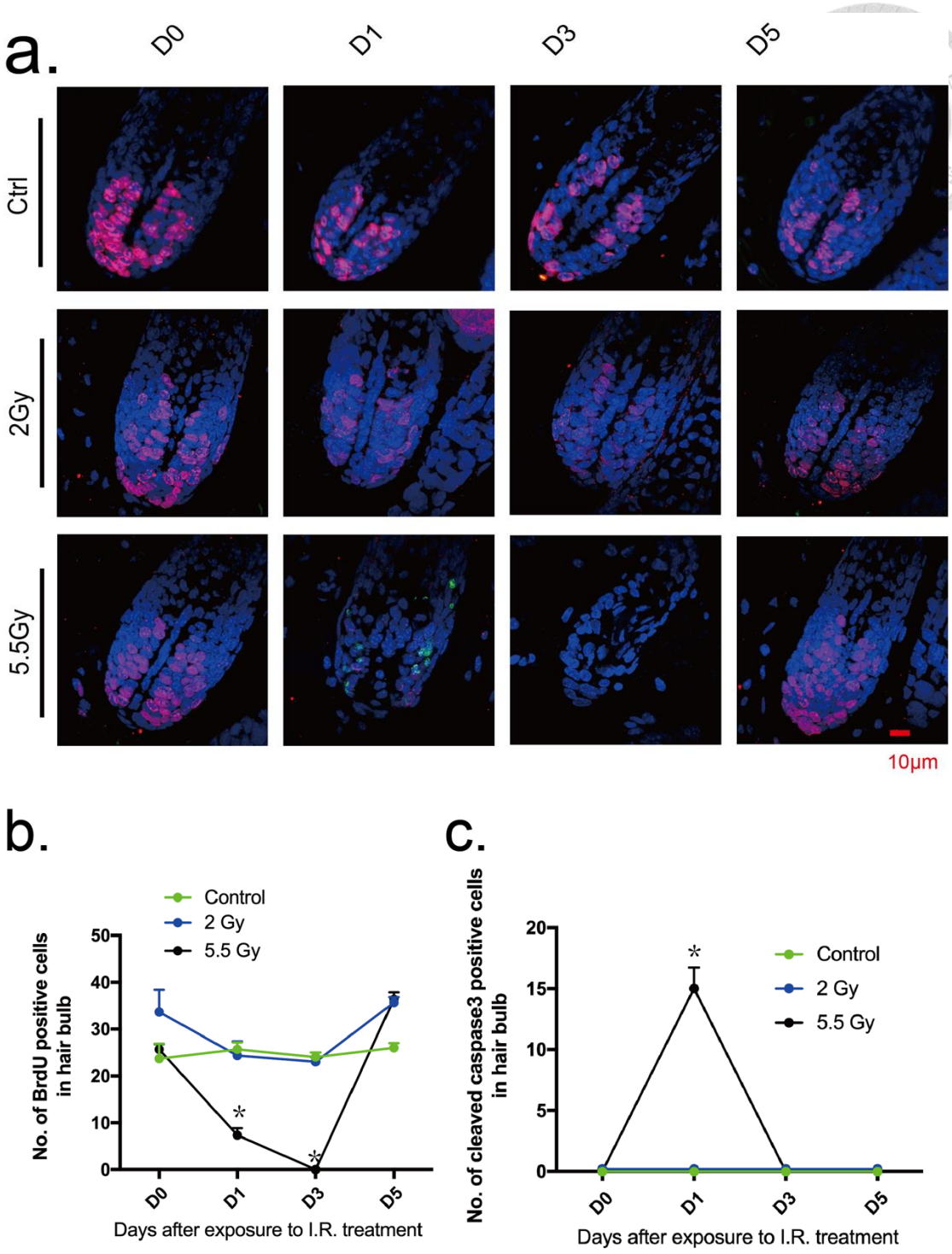

Fig.6 Irradiation induce hair injury in dermal macroenvironment.

(a)Apoptosis and cell proliferation were labelled by cleaved caspase3 and BrdU. (cleaved caspase 3: green; BrdU: red)

(b,c) Statistics of HFs injury and proliferation induced by I.R. treatment.

doi:10.6342/NTU201901903

3.4 Dermal macroenvironment respond to ionizing radiation

Adipose tissue contains immune cells, adipocytes, extracellular matrix, fibroblasts, vascular cells, neuronal cells and stromal cells.(Lago, Cerqueira et al. 2018) There were various degree injury induced by distinct radiation dosage. Thus, we were trying to figure out dermal macroenvironment injury induced by radiation. Oil red O staining results showed that lipid droplet and adipocytes buckling at post-5.5Gy I.R. day3 to day5 and post-2Gy I.R. day3(Fig.7a). This result inferred that lipid droplet and adipocytes were sensitive to radiation. As illustrated by Fig.7b, ORO positive cells in dermis significantly increased after post-5.5Gy I.R. day3 to day5 and only increased at post-2Gy I.R. day3. However, we used masson trichome staining to identify phenotype of collagen fibers and muscle fibers after exposure to radiation as could be found in Fig.7c. This result demonstrated that collagen fibers were destroyed after exposure to 2Gy and 5.5Gy radiation. We assumed that collagen fibers were highly sensitive to radiation treatment. In addition, we used F4/80 immuno-marker to identify immune infiltration caused by radiation.(Fig.7d) We found that amount of macrophages significantly after exposure to 2Gy and 5.5Gy I.R decreased then increased later on .

doi:10.6342/NTU201901903

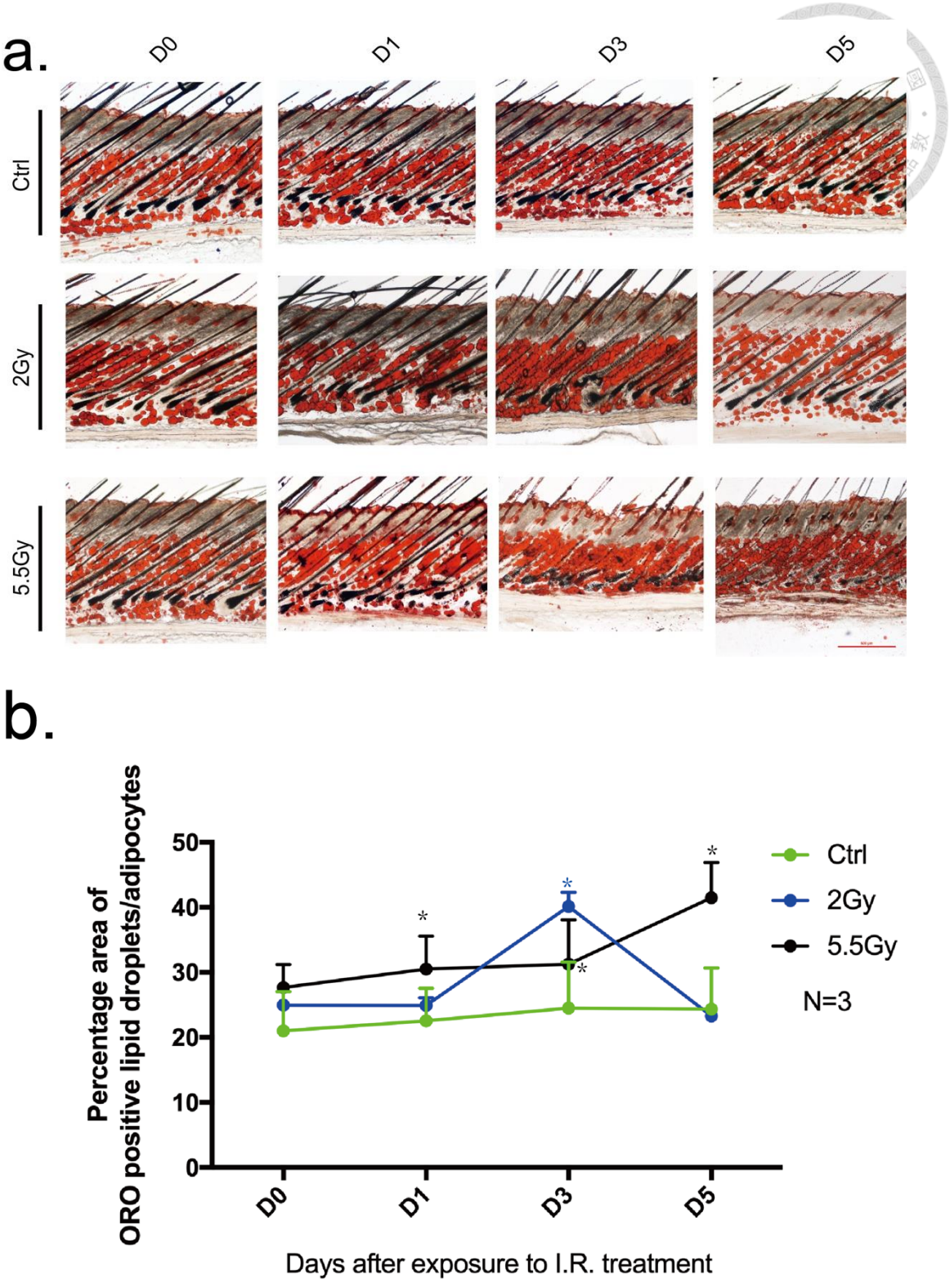

Fig.7 Dermal macroenvironment changed response to I.R. treatment

(a) lipid droplet buckling in dermal macroenvironment. Lipid droplet would decrease significantly at post-5.5Gy I.R.

(b) Statistics of ORO staining of lipid droplet rand adipocytes response to I.R. treatment

doi:10.6342/NTU201901903

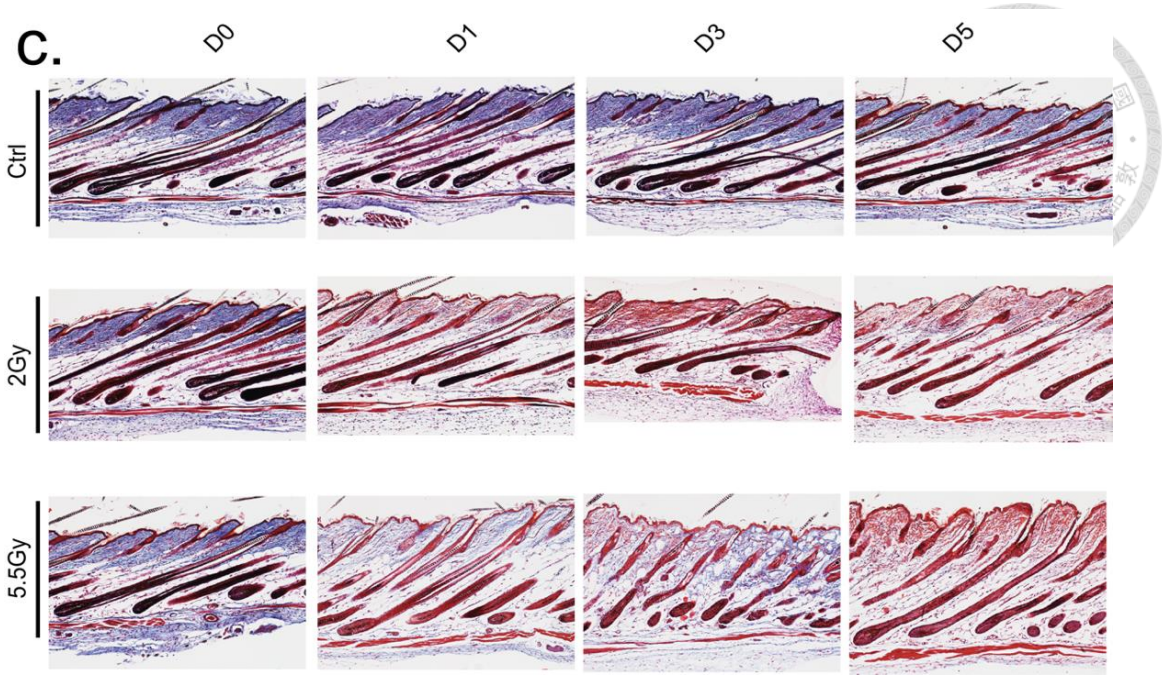

(c) Masson trichome staining in dermal macroenvironment and HFs.(collagen: blue, muscle fibers: red, nuclei: black/blue) This result indicated that the muscle fiber in dermal macroenvironment will significantly decrease at post-5.5Gy I.R. treatment.

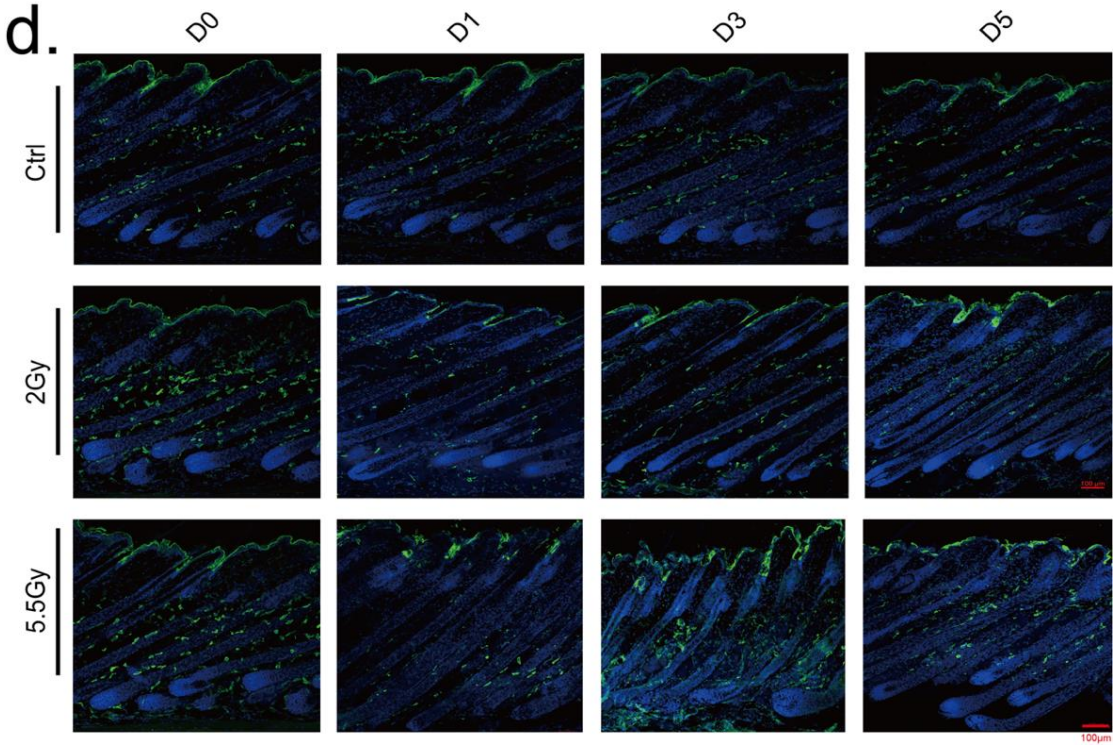

(d) F4/80 immunostaining in dermal macroenvironment and HFs.(green:F4/80; blue: Hoechst) After 2Gy/ 5.5Gy I.R. treatment, macrophage significantly decrease in dermal macroenvironment.

doi:10.6342/NTU201901903

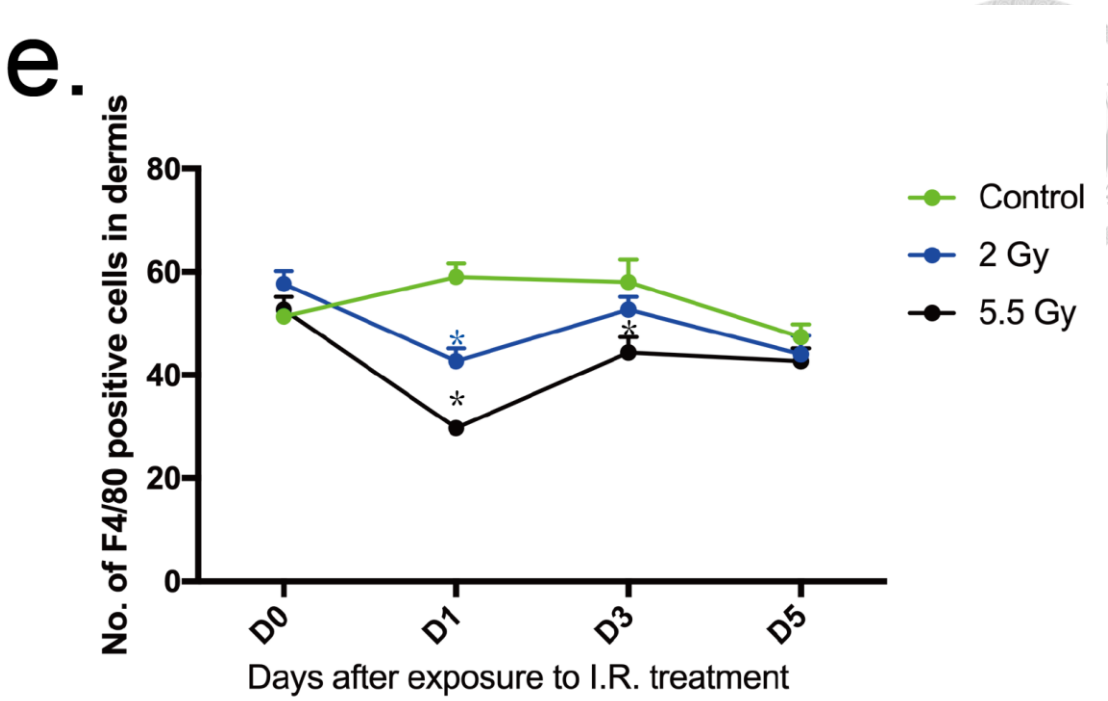

(e) Statistics of F4/80 immunostaining positive cells of dermal macroenvironment and HFs after exposure to I.R. treatment.

doi:10.6342/NTU201901903

3.5 Profiling distinction between each radiation dosage treatment population from total proteome

To profile exhaustive total proteome result from each radiation treatment, we focused on the significant change protein population in 6hrs and 24hrs after exposure to radiation treatment. By the label-free technique, in 2Gy radiation treatment, there were 3585 proteins ID been identified and 1497 significant changed protein ID analysis by ANOVA. In 5.5Gy radiation treatment, there were 3585 proteins ID been identified and 1804 significant changed protein ID analysis by ANOVA. There were more total of significant change proteins ID in 5.5Gy radiation treatment compared to 2Gy radiation treatment. We identified 232 proteins enriched only in 2Gy radiation, 539 proteins enriched only in 5.5Gy radiation and 1263 proteins enriched in both population.(Fig.8a) By GO terms analysis towards the both proteins population, the oxidation-reduction process related proteins was the most significant enriched in 2Gy and 5.5Gy I.R. (Fig.8c) We discovered that there were the others different biological process GO terms which were enriched, including platelet related function activity, cell homeostasis, ATP metabolism etc. As listed in Fig.8b, this result indicated that triglyceride metabolic process and glucose metabolic process would have up-regulated expression level by 5.5Gy I.R. stimulation but down-regulated expression

doi:10.6342/NTU201901903

level by 2Gy I.R. stimulation. In addition, the transcription and translation related GO terms ranked ahead as detailed in Fig.8d.

doi:10.6342/NTU201901903

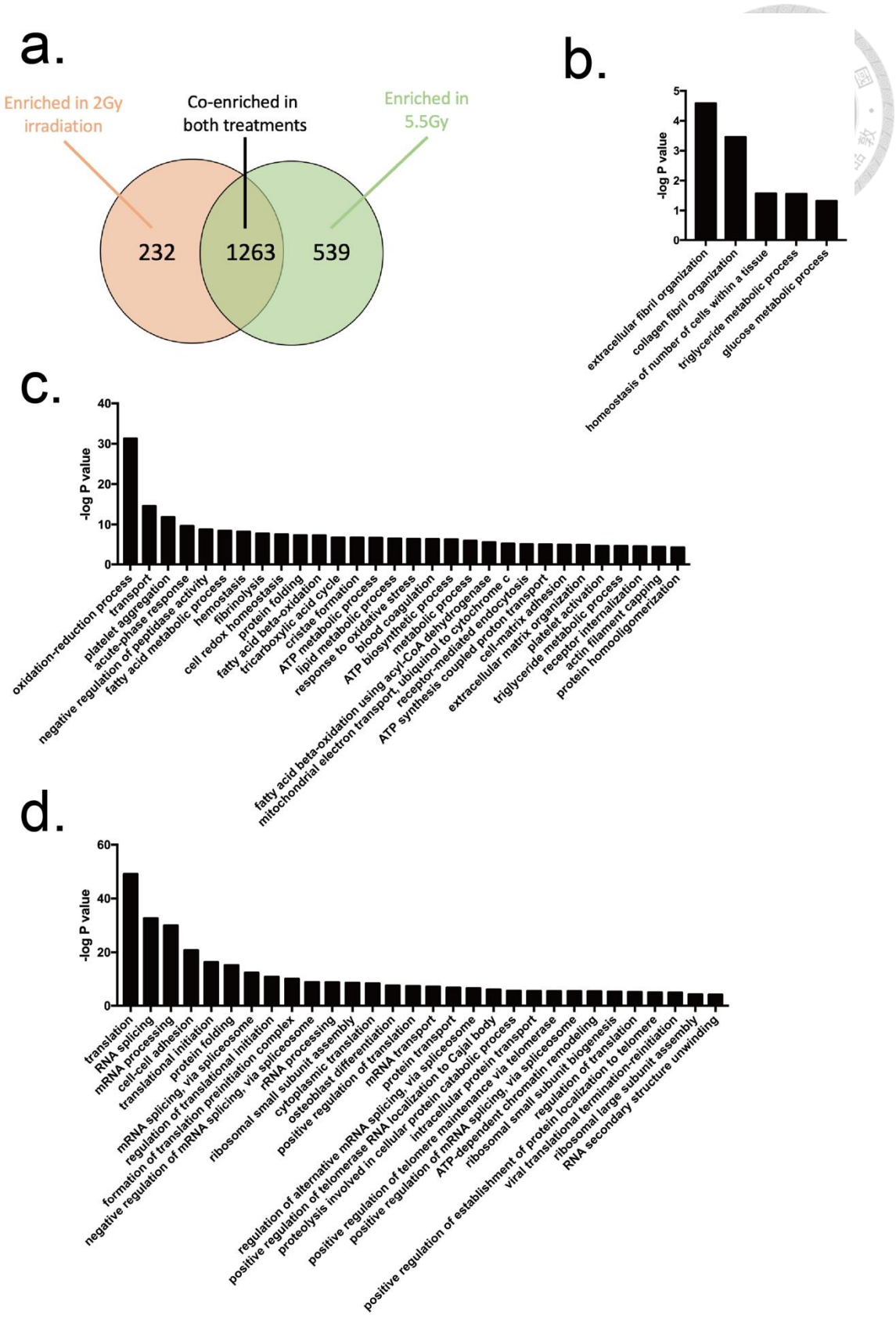

doi:10.6342/NTU201901903

Fig.8 Significant changed proteins ID by ANOVA analysis. Significantly enriched Gene Ontology (GO) terms according to DAVID bioinformatics resources.

(a) Enriched proteins populations in 2Gy and 5.5Gy.

(b) Up-regulated expression levels of significant protein enriched in 5.5Gy but down-regulated expression level in 2Gy

(c) Top30 up-regulated expression levels of significant protein enriched in 2Gy and 5.5Gy

(d) Up-regulated expression levels of significant protein enriched in 2Gy but down-regulated expression level in 5.5Gy

doi:10.6342/NTU201901903

3.6 Comparing the proteome in each population

By same strategy, we identified the GO terms in biological process only expressed in single I.R. dosage. Firstly, there were 232 enriched proteins only expressed in 2Gy I.R.(Fig.8a) These GO terms were highly expressed in biological process of cell-cell adhesion, endocytosis and protein transport. (Fig.9a) We speculated that cell-cell adhesion and endocytosis responsed to cell apoptosis signal induced by radiation injury in dermal macroenvironment and HFs. However, there were 539 enriched proteins only expressed in 5.5Gy I.R..(Fig.8a) These GO terms were highly expressed in biological process of muscle contraction.(Fig.9b) This result matched the Masson trichome staining showing that muscle related protein had changed significantly.(Fig.7c) We hypothesized that if dermal macroenvironment and HFs received higher I.R. it would perform supplemental energy activity such as oxidation reduction process and tricarboxylic acid cycle. The cell-cell adhesion related GO terms were co-enriched in two radiation dosage population, but it included different protein markers in each population. In Fig.9c, we identified certain cell-cell adhesion related proteins that were up-regulated and enriched only in 5.5Gy I.R. , such as Glod4, Pdlim5, Prdx1, Vabp, Capzb, Paics. By contrast, there were another cell-cell adhesion re;ated proteins markers which were down regulated and enriched only in 5.5Gy I.R., such as Twf1, Hdlbp, Ywhab, Ahsa1, Sfn, Eefld, Eif4h, Eif4g2,

doi:10.6342/NTU201901903

Gigyf2, Twhaz, Vasp, Capzb, Stat1, Ldha and Larp1. In the previous study, Ldha, protein marker was highly corelated to hair follicle stem cell activity.(Flores, Schell et al. 2017) It could be inferred that expression level of Ldha in hair follicle stem cell was sensitive to radiation and highly correlated to hair follicle regeneration. In Fig. 9d, we found that cell-cell adhesion related proteins that were up-regulated and enriched only in 2Gy I.R. , such as Scrib, Ndrg1, Snx9, Sh3g11, Mprip, Stk24, Snx5, Ppplr131, Esyt2, Fscn1, Hist1h3a, Arfip1, Gipc1, Ist1. In the previous study, Scrib, this protein marker would mediate epidermal development and played a role of tumor suppressive function in skin.(Pearson, McGlinn et al. 2015) It could be assumed that radiation might affect tumor suppressive function and increased expression level.

doi:10.6342/NTU201901903

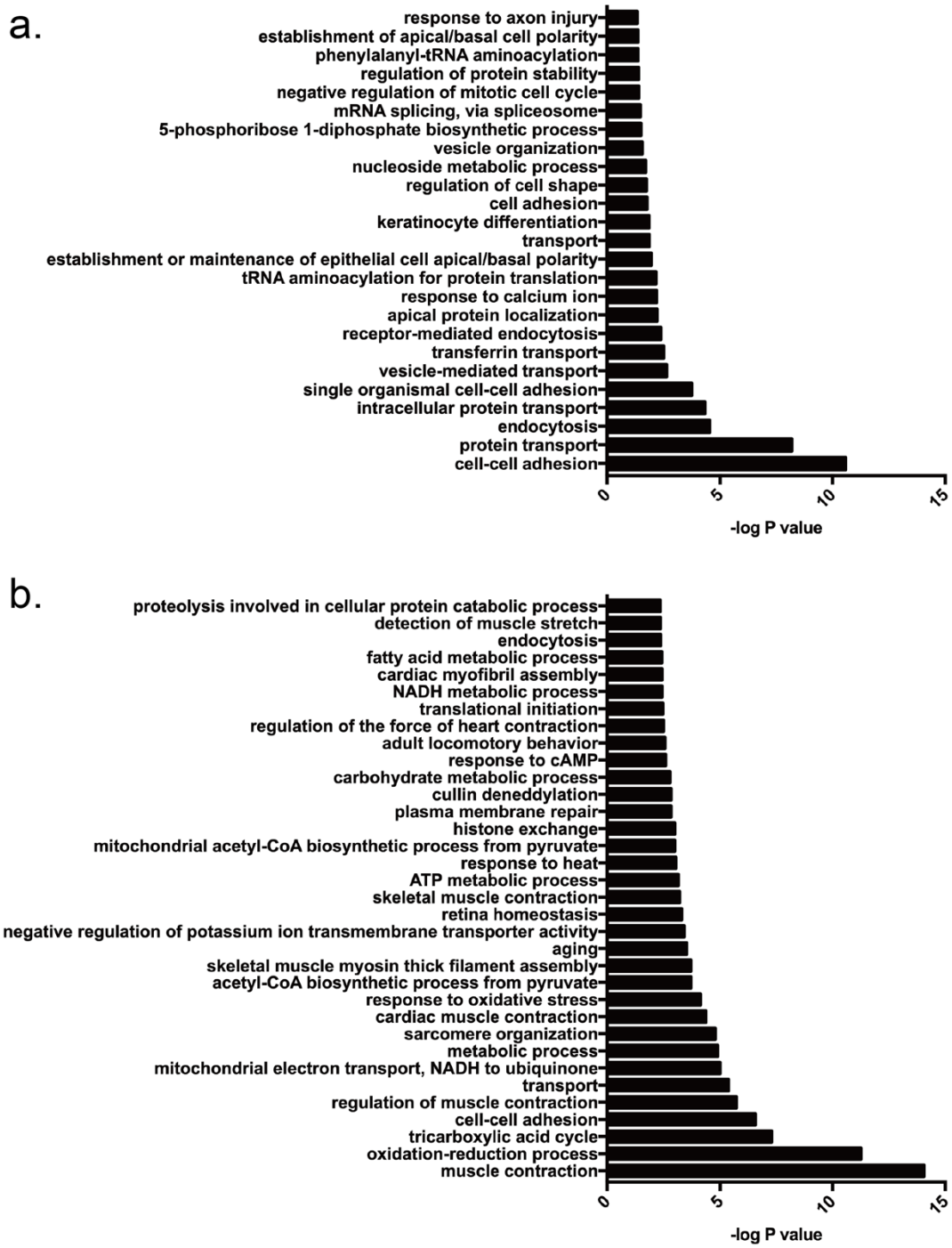

Fig.9 Enriched GO term in biological process

(a) GO term in biological process only expressed in 2Gy radiation

(b) GO term in biological process only expressed in 5.5Gy radiation

doi:10.6342/NTU201901903

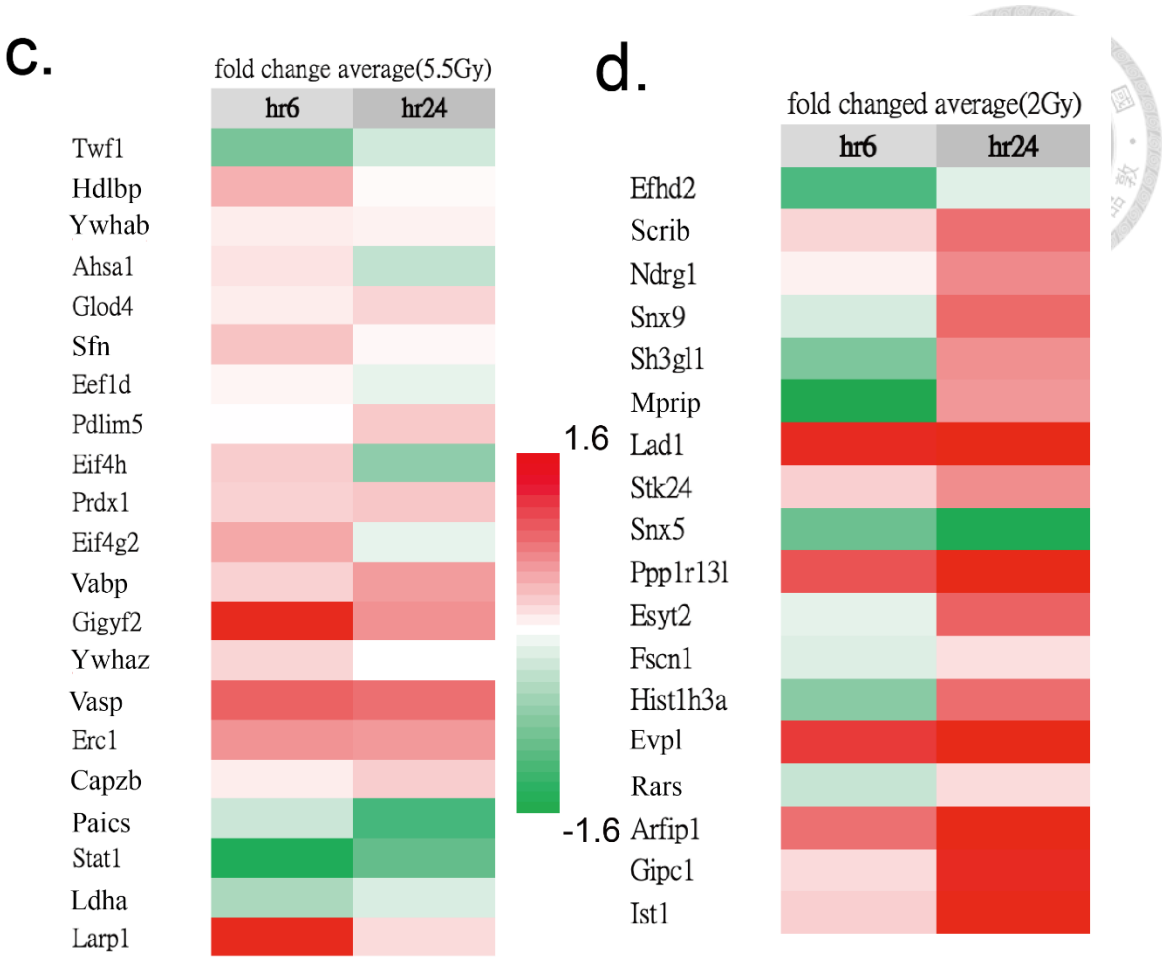

(c) Identified protein markers hit in cell-cell adhesion related GO term which were enriched in different radiation dosage population

doi:10.6342/NTU201901903

3.7 Fat metabolism related biological process were highly enriched in both population

As can be seen in Fig.8c, the ranking of oxidation-reduction process was the most significant GO term in top 30 up-regulated expression level in 2Gy and 5.5Gy. This result revealed that fat metabolism related GO terms included fatty acid metabolic process, fatty acid beta-oxidation, lipid metabolic process, fatty acid beta-oxidation using acyl-CoA dehydrogenase, and triglyceride metabolic process. This result matched the previous data at Fig.7a, fat metabolism related protein would have dramatically changed after exposure to I.R. treatment. Here, we used the enriched proteins ID in fat metabolism related protein (Fig.8c) to figure out the correlation of fat metabolism. (Fig.10) This figure indicated that our fat metabolism related protein were highly expressed correlated to fatty acid beta-oxidation and lipid metabolism.

doi:10.6342/NTU201901903

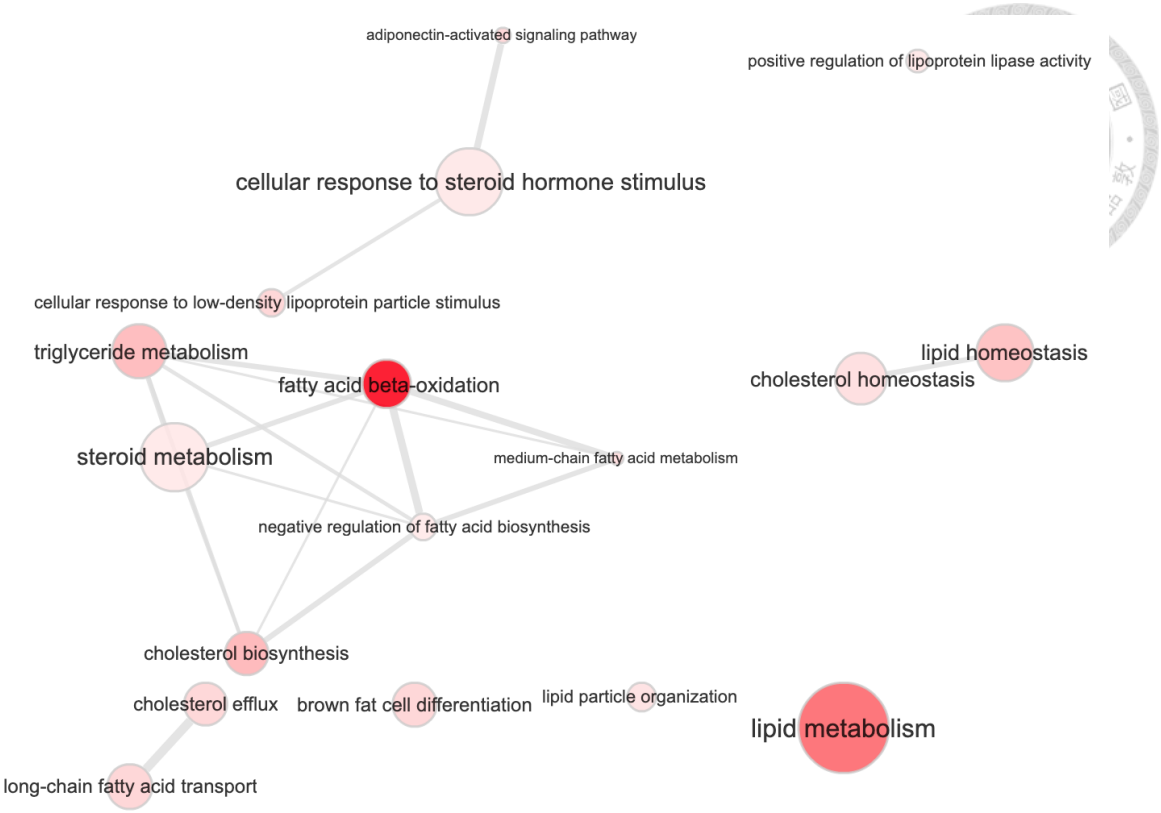

Fig.10 Fat metabolism GO terms were enriched in both radiation dosage.

doi:10.6342/NTU201901903

3.8 Lipolysis inhibition delayed the recovery of hair re-entry anagen stage after I.R. injury

To examine the response of anagen HFs to I.R. injury with lipolysis inhibition, we tested the hypothesis that lipolysis induced by I.R. in dermal macroenvironment would affect recovery of HFs after I.R. treatment in mice. We used 32-day-old mice receiving I.R. with or without Acipimox oral intake in the following 25 days and found significant results. As can be seen in Fig.11c,it is apparent that if mice receive I.R. treatment with Acipimox oral intake, HFs will delay anagen stage until much later. In addition, body weights data in Fig.11d indicated that there was no difference between group of receiving Acipimox intake or non-intake control group after I.R. treatment. As shown in Fig.11a, if mice received I.R. treatment without Acipimox, HFs will enter anagen stage at post-I.R. day28. In contrast, if mice receive I.R. treatment with Acipimox, HFs will enter anagen stage at post-I.R. day 39. (Fig.11b) Comparing Fig.11a and Fig.11b showed that HFs delayed re-entry anagen stage by almost 10days after I.R. treatment depending on whether the mice receiving Acipimox oral intake. The degree of I.R. injury to HFs could be inspected by histological examination, proving that lipolysis inhibition system protected structure of hair matrix intact than without receiving Acipimox intake with I.R. treatment.(Fig. 11e) As indicated in Fig.11f, it seemed that lipolysis inhibition with I.R. treatment would prolong catagen of hair cycle until post-I.R. day13 . However, mice did not received Acipimox with I.R. treatment which would entered telogen stage at post-I.R. day11. As can be seen in Fig.11g, we found that mice receiving I.R. treatment without Acipimox would entered full anagen stage at day30. But mice receiving I.R. treatment with Acipimox remained in telogen. In Fig.11h, it seemed that mice receiving I.R. treatment with Acipimox entered full anagen stage at post-I.R. day41 to 45. However,

doi:10.6342/NTU201901903

mice receiving I.R. treatment without Acipimox remained full anagen stage until post-I.R. day 43 and turned into catagen stage at post-I.R. day 45. Whether mice receiving I.R. with Acipimox oral intake or not, all returned to normal postnatal hair cycle regeneration at post-I.R. day41.

doi:10.6342/NTU201901903

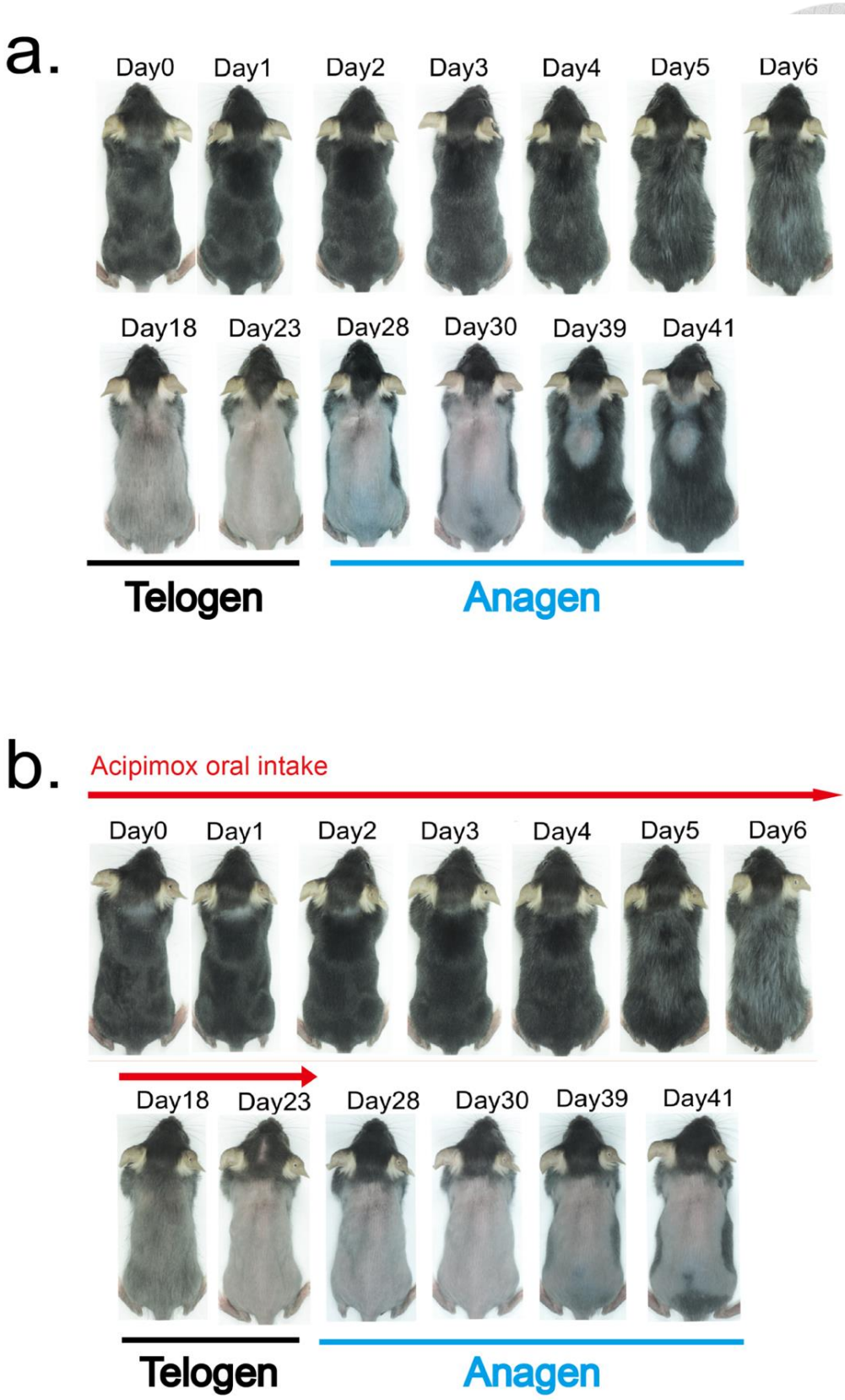

Fig.11 Lipolysis inhibition would delayed hair growth after I.R. treatment.
(a,b) Gross view indicated that HFs delayed re-entry anagen stage almost 10days after I.R. treatment whether the mice receiving Acipimox oral intake

doi:10.6342/NTU201901903

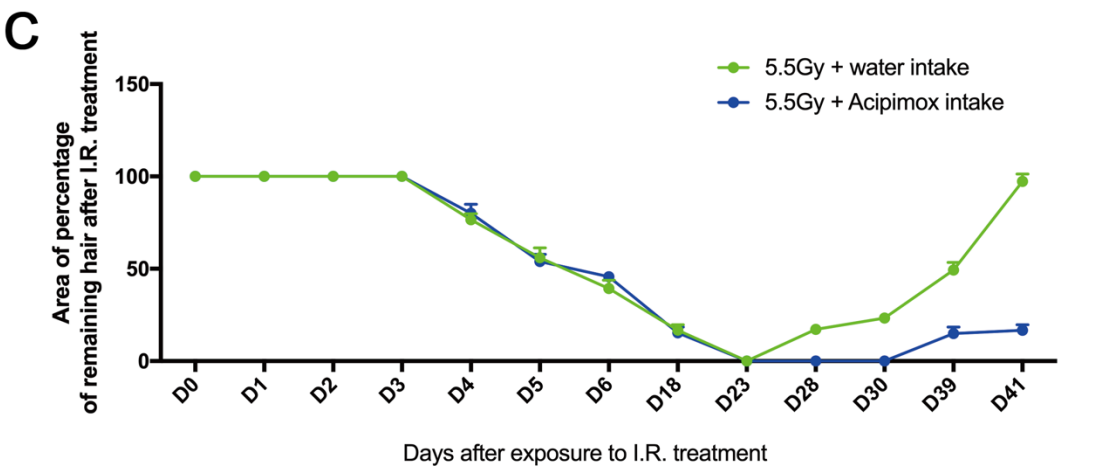

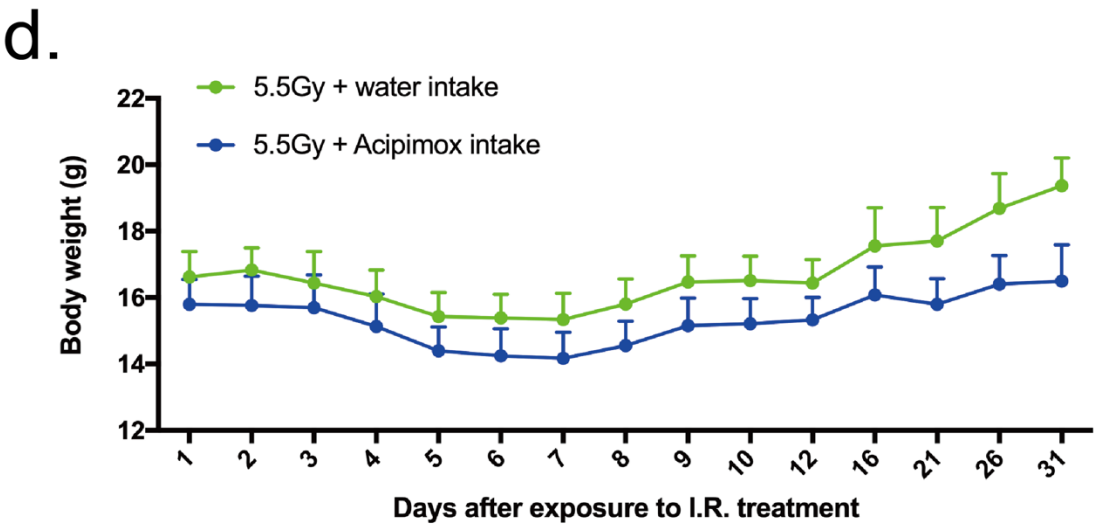

(c) Hair growth score for 41days after exposure to 5.5Gy ionizing radiation with Acipimox oral intake or water intake. This result revealed that Acipimox will delayed hair growth re-entry anagen

(d) Body weights of mouse for 31 days. Acipimox oral intake did not change body weight.

doi:10.6342/NTU201901903

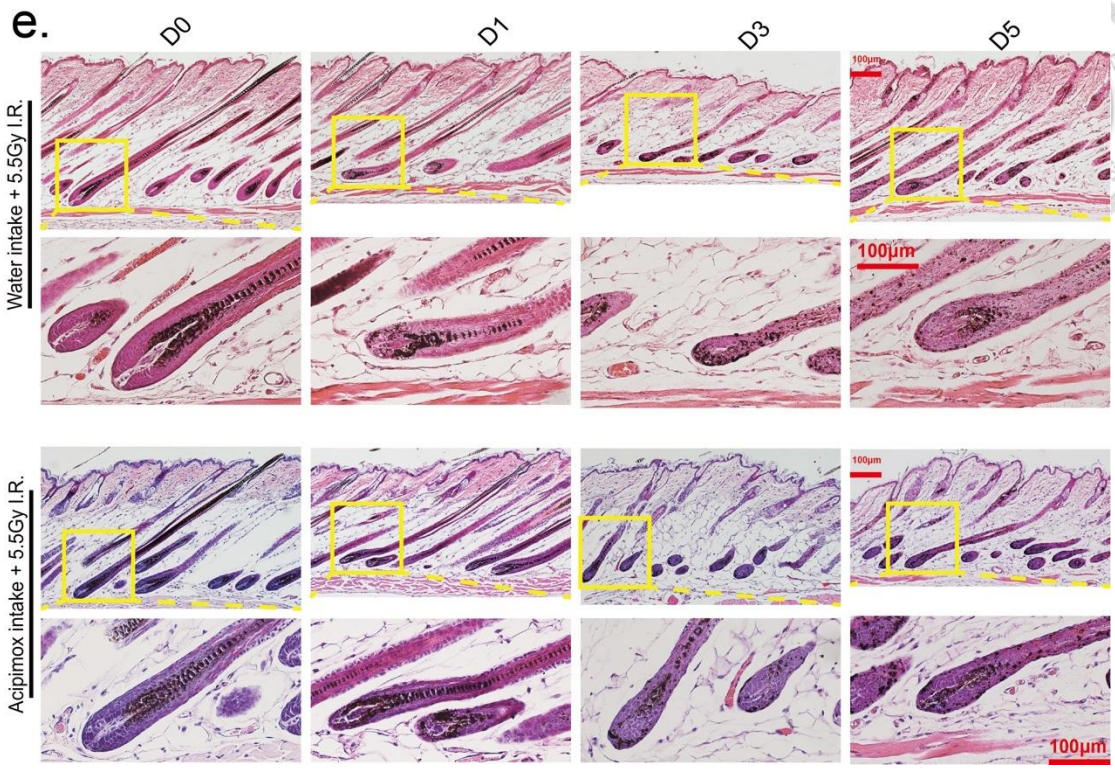

(e) Histology examination of combination of 5.5Gy and water intake, combination of 5.5Gy and Acipimox oral intake at day0 to day5. This result revealed that structure of hair matrix in Acipimox oral intake group was more intact than water oral intake group undergoes.

doi:10.6342/NTU201901903

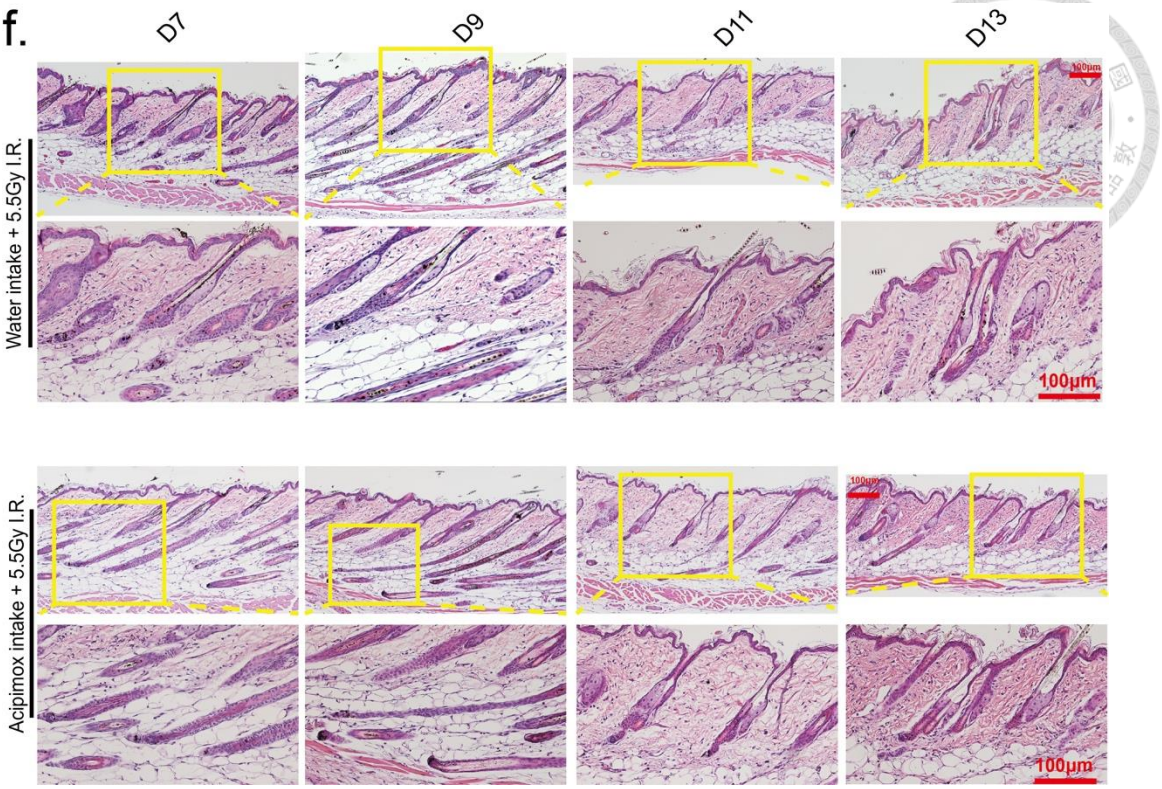

(f) Histology examination of combination of 5.5Gy and water intake, combination of 5.5Gy and Acipimox oral intake at day7 to day13. This result revealed that lipolysis inhibition with I.R. treatment would prolonged catagen stage.

doi:10.6342/NTU201901903

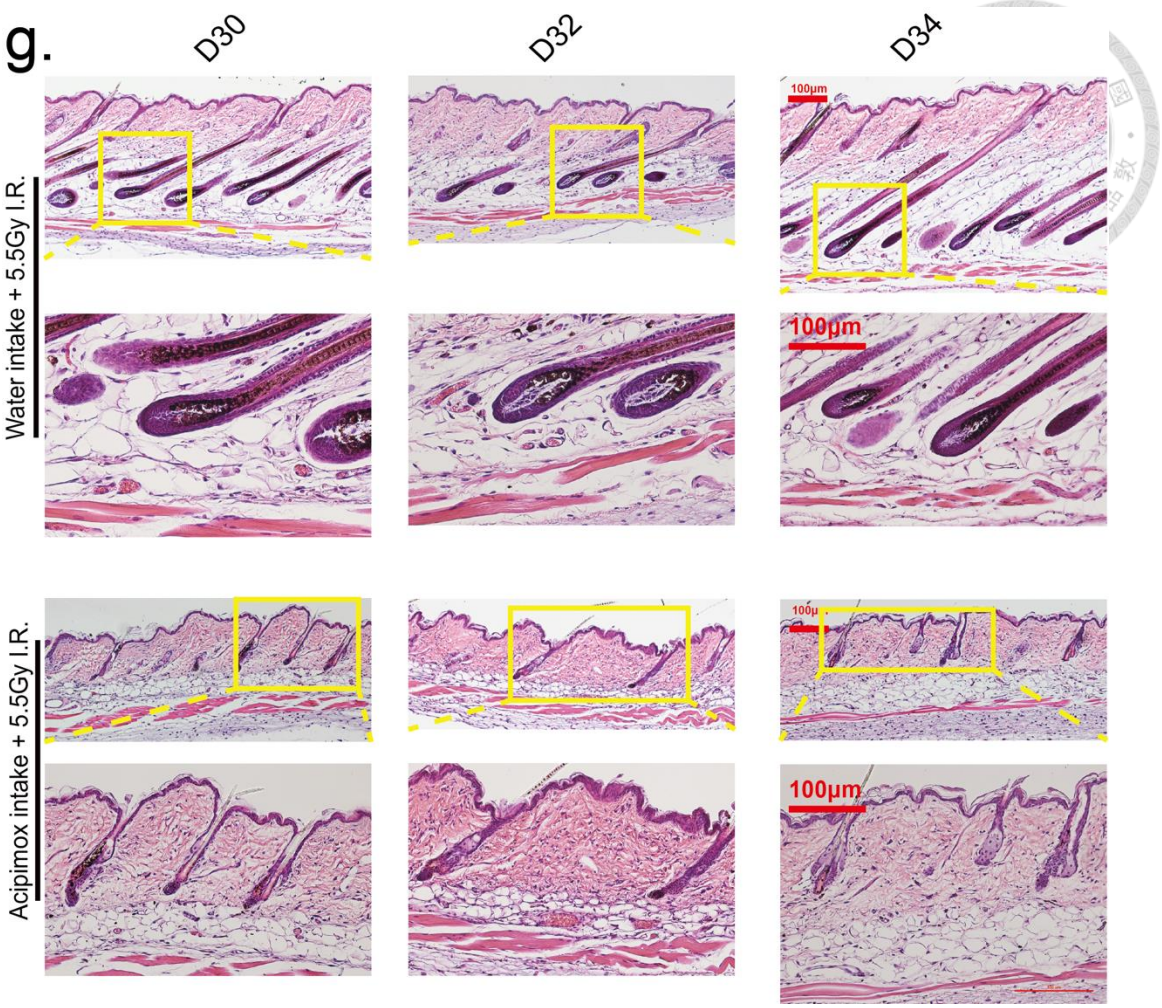

(g) Histology examination of combination of 5.5Gy and water intake, combination of 5.5Gy and Acipimox oral intake at day30 to day34. This result revealed that lipolysis inhibition with I.R. treatment would prolonged catagen stage.

doi:10.6342/NTU201901903

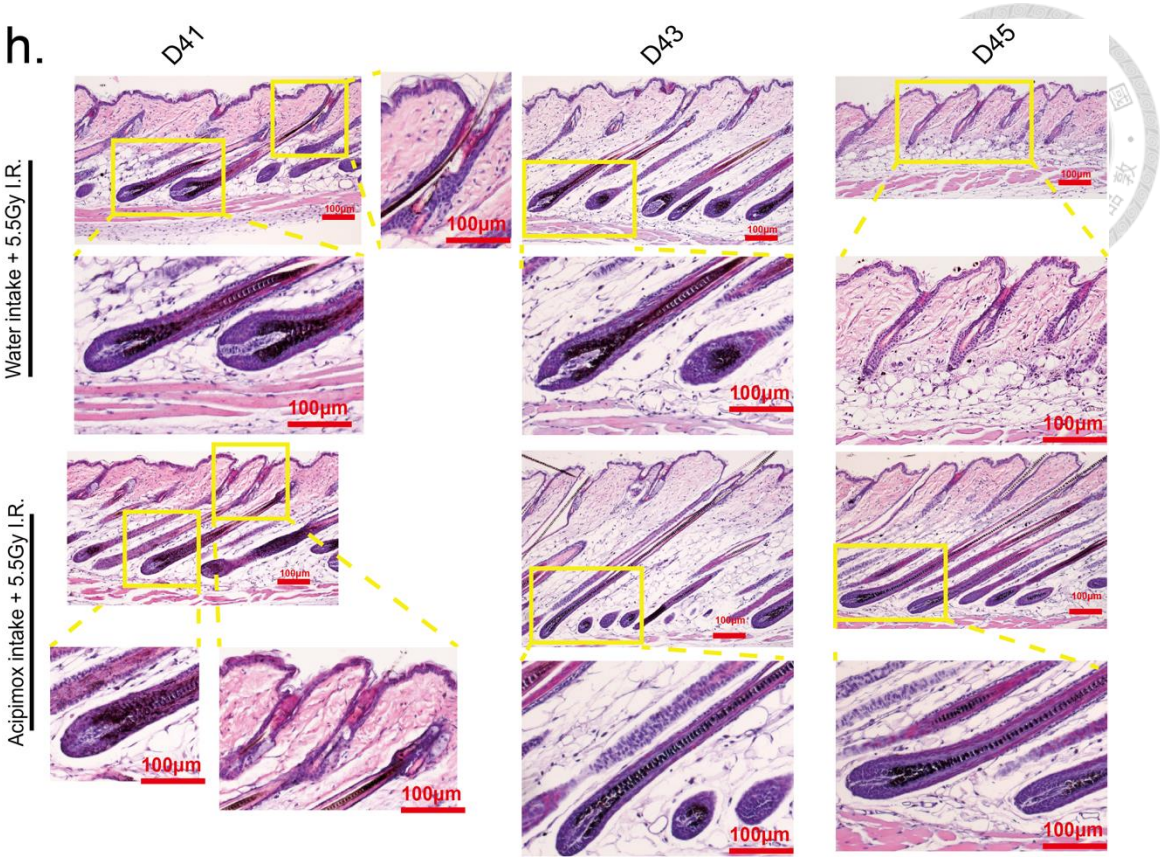

(h) Histology examination of combination of 5.5Gy and water intake, combination of 5.5Gy and Acipimox oral intake at day41 to day45. This result revealed that lipolysis inhibition with I.R. treatment would prolonged catagen stage.

doi:10.6342/NTU201901903

Chapter 4 Discussion and conclusions

Thus far we have investigated dermal macroenvironment and hair follicle after radiation treatment by immunofluorescence staining, H&E staining, masson trichome staining. From the results above, we can see some evidence about synchronized change of dermal macroenvironment and HFs induced by radiation treatment. These evidences provide us useful clues to indicate that interacted regulation of hair regeneration and dermal macroenvironment have strong correlation.

From proteomic analysis results, it provided more details to characterize the HFs and dermal macroenvironment at various cell status undergoing radiation treatment. According to proteins ID that underwent significant changes, we can get more information about the radiation stimuli induced cross-talk from dermal macroenvironment and hair follicle's intrinsic protein network. This network might highly correlate with mitochondria, this hypothesis was based on the result(Fig. 8b) which indicated that many GO terms occurred in mitochondria.

On the other hand, we used a lipolysis inhibitor, Acipimox as our functional assay to inducee lowered the triglyceride levels in mice. We hypothesized thtat this drug could also lower fatty acid release through lowered level of triglyceride. In our study, combination of Acipimox oral intake and 5.5Gy I.R. treatment group would delayed re-entry anagen stage almost 10 days. Our lipolysis inhibition with I.R.

doi:10.6342/NTU201901903

treatment results were in general agreement with previous dermal white adipose tissue induced hair follicle cycle studies in mice.(Foster, Nicu et al. 2018) However, the lipolysis inhibition mechanism underlying radiation treatment remains unclear. This mechanism could eventually lead to a new biomarkers with radiation treatment.

doi:10.6342/NTU201901903

Chapter 5 Reference

1. A. Urruticoechea, R. A., J. Balart, A. Villanueva, F. Viñals and G. Capellá (2010). "Recent Advances in Cancer Therapy- An Overview."
2. Alonso, L. and E. Fuchs (2006). "The hair cycle." J Cell Sci **119**(Pt 3): 391-393.
3. Arnold Biological Luboratory, B. U., Providence, Rhode Island (1953). "Changes in the skin relation to the hair growth cycle."
4. Balagamwala, E. H., A. Stockham, R. Macklis and A. D. Singh (2013). "Introduction to radiotherapy and standard teletherapy techniques." Dev Ophthalmol **52**: 1-14.
5. Baskar, R., K. A. Lee, R. Yeo and K. W. Yeoh (2012). "Cancer and radiation therapy: current advances and future directions." Int J Med Sci **9**(3): 193-199.
6. Bentzen, S., W. Dorr, M. Anscher, J. Denham, M. Hauerjensen, L. Marks and J. Williams (2003). "Normal tissue effects: reporting and analysis." Seminars in Radiation Oncology **13**(3): 189-202.
7. Bentzen, S. M. (2006). "Preventing or reducing late side effects of radiation therapy: radiobiology meets molecular pathology." Nat Rev Cancer **6**(9): 702-713.
8. Brown, A. and H. Suit (2004). "The centenary of the discovery of the Bragg peak." Radiother Oncol **73**(3): 265-268.
9. Chase, H. B. (1954). "Growth of the Hair."
10. Cox, J. and M. Mann (2008). "MaxQuant enables high peptide identification rates, individualized p.p.b.-range mass accuracies and proteome-wide protein quantification." Nat Biotechnol **26**(12): 1367-1372.
11. Davis, B. K. (1962). "Mechanism of hair-growth.pdf>."
12. De Ruysscher, D., G. Niedermann, N. G. Burnet, S. Siva, A. W. M. Lee and F. Hegi-Johnson (2019). "Radiotherapy toxicity." Nat Rev Dis Primers **5**(1): 13.
13. Delaney, G., S. Jacob, C. Featherstone and M. Barton (2005). "The role of radiotherapy in cancer treatment: estimating optimal utilization from a review of evidence-based clinical guidelines." Cancer **104**(6): 1129-1137.
14. Donya, M., M. Radford, A. ElGuindy, D. Firmin and M. H. Yacoub (2014). "Radiation in medicine: Origins, risks and aspirations." Glob Cardiol Sci Pract **2014**(4): 437-448.
15. Driskell, R. R., C. Clavel, M. Rendl and F. M. Watt (2011). "Hair follicle dermal papilla cells at a glance." J Cell Sci **124**(Pt 8): 1179-1182.
16. Driskell, R. R., C. A. Jahoda, C. M. Chuong, F. M. Watt and V. Horsley (2014). "Defining dermal adipose tissue." Exp Dermatol **23**(9): 629-631.

doi:10.6342/NTU201901903

17. F.D. Malkinsonm, L. G. R. M. (1972). "Effects Of Hydroxyurea And Radiation On Hair Matrix Cells."
18. Festa, E., J. Fretz, R. Berry, B. Schmidt, M. Rodeheffer, M. Horowitz and V. Horsley (2011). "Adipocyte lineage cells contribute to the skin stem cell niche to drive hair cycling." Cell **146**(5): 761-771.
19. Flores, A., J. Schell, A. S. Krall, D. Jelinek, M. Miranda, M. Grigorian, D. Braas, A. C. White, J. L. Zhou, N. A. Graham, T. Graeber, P. Seth, D. Evseenko, H. A. Coller, J. Rutter, H. R. Christofk and W. E. Lowry (2017). "Lactate dehydrogenase activity drives hair follicle stem cell activation." Nat Cell Biol **19**(9): 1017-1026.
20. Foitzik, K., K. Krause, F. Conrad, M. Nakamura, W. Funk and R. Paus (2006). "Human scalp hair follicles are both a target and a source of prolactin, which serves as an autocrine and/or paracrine promoter of apoptosis-driven hair follicle regression." Am J Pathol **168**(3): 748-756.
21. Formenti, S. C. and S. Demaria (2009). "Systemic effects of local radiotherapy." The Lancet Oncology **10**(7): 718-726.
22. Foster, A. R., C. Nicu, M. R. Schneider, E. Hinde and R. Paus (2018). "Dermal white adipose tissue undergoes major morphological changes during the spontaneous and induced murine hair follicle cycling: a reappraisal." Arch Dermatol Res **310**(5): 453-462.
23. Franklin H. Epstein, M. D. (1999). "The biology of hair follicles."
24. GerdLindner, V. B., Natalia V. Botchkareva, Gao Ling, Carinavan derVeen,andRalfPaus (1997). "Analysis of Apoptosis during Hair Follicle Regression (Catagen)."
25. Greco, V., T. Chen, M. Rendl, M. Schober, H. A. Pasolli, N. Stokes, J. Dela Cruz-Racelis and E. Fuchs (2009). "A two-step mechanism for stem cell activation during hair regeneration." Cell Stem Cell **4**(2): 155-169.
26. Hardy, M. H. (1992). "<The secret life of the hair follicle.pdf>."
27. Herman B. Chase, H. R. a. V. W. S. (1951). "Critical Stages of Hair Development and Pigmentation in the Mouse."
28. Huang, W. Y., S. F. Lai, H. Y. Chiu, M. Chang, M. V. Plikus, C. C. Chan, Y. T. Chen, P. N. Tsao, T. L. Yang, H. S. Lee, P. Chi and S. J. Lin (2017). "Mobilizing Transit-Amplifying Cell-Derived Ectopic Progenitors Prevents Hair Loss from Chemotherapy or Radiation Therapy." Cancer Res **77**(22): 6083-6096.
29. Kwok, K. H., K. S. Lam and A. Xu (2016). "Heterogeneity of white adipose tissue: molecular basis and clinical implications." Exp Mol Med **48**: e215.
30. Lago, M. E. L., M. T. Cerqueira, R. P. Pirraco, R. L. Reis and A. P. Marques (2018). Skin in vitro models to study dermal white adipose tissue role in skin

doi:10.6342/NTU201901903

healing. Skin Tissue Models for Regenerative Medicine**:** 327-352.
31. Mehta, S. R., V. Suhag, M. Semwal and N. Sharma (2010). "Radiotherapy: Basic Concepts and Recent Advances." Medical Journal Armed Forces India **66**(2): 158-162.
32. Muller-Rover, S., B. Handjiski, C. van der Veen, S. Eichmuller, K. Foitzik, I. A. McKay, K. S. Stenn and R. Paus (2001). "A comprehensive guide for the accurate classification of murine hair follicles in distinct hair cycle stages." J Invest Dermatol **117**(1): 3-15.
33. Paus, K. S. S. A. R. (2001). "Controls of hair follicle cycling."
34. Paus, R., I. S. Haslam, A. A. Sharov and V. A. Botchkarev (2013). "Pathobiology of chemotherapy-induced hair loss." The Lancet Oncology **14**(2): e50-e59.
35. Pawlik, T. M. and K. Keyomarsi (2004). "Role of cell cycle in mediating sensitivity to radiotherapy." Int J Radiat Oncol Biol Phys **59**(4): 928-942.
36. Pearson, H. B., E. McGlinn, T. J. Phesse, H. Schluter, A. Srikumar, N. J. Godde, C. B. Woelwer, A. Ryan, W. A. Phillips, M. Ernst, P. Kaur and P. Humbert (2015). "The polarity protein Scrib mediates epidermal development and exerts a tumor suppressive function during skin carcinogenesis." Mol Cancer **14**: 169.
37. Porter AG1, J. R. (1999). "Emerging roles of caspase-3 in apoptosis."
38. Schneider, M. R., R. Schmidt-Ullrich and R. Paus (2009). "The hair follicle as a dynamic miniorgan." Curr Biol **19**(3): R132-142.
39. Schulz-Ertner, D., O. Jakel and W. Schlegel (2006). "Radiation therapy with charged particles." Semin Radiat Oncol **16**(4): 249-259.
40. Stenn KS, N. A., Jahoda CAB, McKay IA, Paus R (1999). "What controls hair follicle cycling."
41. Teruhiko Terasawa, M. T. D., MD; Stanley Ip, MD; Gowri Raman, MD; Joseph Lau, MD; and Thomas A. Trikalinos, MD, PhD (2009). "Systematic Review: Charged-Particle Radiation Therapy for Cancer."
42. Yang, H., R. C. Adam, Y. Ge, Z. L. Hua and E. Fuchs (2017). "Epithelial-Mesenchymal Micro-niches Govern Stem Cell Lineage Choices." Cell **169**(3): 483-496 e413.
43. Zwick, R. K., C. F. Guerrero-Juarez, V. Horsley and M. V. Plikus (2018). "Anatomical, Physiological, and Functional Diversity of Adipose Tissue." Cell Metab **27**(1): 68-83.

doi:10.6342/NTU201901903